DOI: 10.1002/chem.200600117

Anticancer Cyclometalated $[Au^{III}_m(C^N^C)_mL]^{n+}$ Compounds: Synthesis and Cytotoxic Properties

Carrie Ka-Lei Li, Raymond Wai-Yin Sun, Steven Chi-Fai Kui, Nianyong Zhu, and Chi-Ming Che*[a]

Abstract: A series of cyclometalated gold(III) compounds $[Au_m(C^N^C)_mL]^{n+}$ ($m=1$–3; $n=0$–3; HC^N^CH = 2,6-diphenylpyridine) was prepared by ligand substitution reaction of L with N-donor or phosphine ligands. The $[Au_m(C^N^C)_mL]^{n+}$ compounds are stable in solution in the presence of glutathione. Crystal structures of the gold(III) compounds containing bridging bi- and tridentate phosphino ligands reveal the presence of weak intramolecular π···π stacking between the $[Au(C^N^C)]^+$ units. Results of MTT assays demonstrated that the $[Au_m(C^N^C)_mL]^{n+}$ compounds containing nontoxic N-donor auxiliary ligands (**2**) exert anticancer potency comparable to that of cisplatin, with IC_{50} values ranging from 1.5 to 84 μM. The use of [Au(C^N^C)(1-methylimidazole)]$^+$ (**2a**) as a model compound revealed that the gold(III)-induced cytotoxicity occurs through an apoptotic cell-death pathway. The cell-free interaction of **2a** with double-stranded DNA was also examined. Absorption titration showed that **2a** binds to calf-thymus DNA (ctDNA) with a binding constant of 4.5×10^5 dm^3 mol^{-1} at 298 K. Evidence from gel-mobility-shift assays and viscosity measurements supports an intercalating binding mode for the **2a**–DNA interaction. Cell-cycle analysis revealed that **2a** causes S-phase cell arrest after incubation for 24 and 48 hours. The cytotoxicity of **3b**–**g** toward cancer cells ($IC_{50}=0.04$–4.3 μM) correlates to that of the metal-free phosphine ligands ($IC_{50}=0.1$–38.0 μM), with $[Au_2(C^N^C)_2(\mu\text{-dppp})]^{2+}$ (**3d**) and dppp (dppp = 1,2-bis(diphenylphosphino)propane) being the most cytotoxic gold(III) and metal-free compounds, respectively. Compound **3d** shows a cytotoxicity at least ten-fold higher than the other gold(III) analogues; in vitro cellular-uptake experiments reveal similar absorptions for all the gold(III) compounds into nasopharyngeal carcinoma cells (SUNE1) (1.18–3.81 ng/cell; c.f., **3d** = 2.04 ng/cell), suggesting the presence of non-gold-mediated cytotoxicity. Unlike **2a**, both gold(III) compounds [Au(C^N^C)(PPh_3)]$^+$ (**3a**) (PPh_3 = triphenylphosphine) and $[Au_2(C^N^C)_2(\mu\text{-dppp})]^{2+}$ (**3d**) interact only weakly with ctDNA and do not arrest the cell cycle.

Keywords: antitumor agents · bioinorganic chemistry · DNA · gold · ligand effects

Introduction

The success of cisplatin and its derivatives as anticancer agents has stimulated the development of metal-based compounds, including those of gold, for anticancer treatment.[1] In this context, extensive investigations on the biological properties of gold(I) and gold(III) have been reported. The development of gold(III) compounds as potential anticancer agents[2,3] has been hampered by their poor stability in solution. To our knowledge, only very few cytotoxic gold(III) compounds, such as [Au(bipy^c-H)(OH)][PF_6] (bipy^c-H = deprotonated 6-(1,1-dimethylbenzyl)-2,2′-bipyridine),[2a,e] [Au(dmamp)Cl_2] (dmamp = 2-(dimethylaminomethyl)phenyl),[2h] and gold(III) tetraarylporphyrins,[3] have shown significant stability.

The stability of metal compounds is usually enhanced by multidentate chelating ligands. Lippard and co-workers first reported the use of the tridentate terpyridine ligand (terpy) to generate a planar gold(III) metallointercalator.[4] Messori, Orioli, and Coronnello also reported a number of gold(III) compounds containing 6-(1,1-dimethylbenzyl)-2,2′-bipyridine ligands.[2a,e] Guo and co-workers recently reported the syn-

[a] C. K.-L. Li, Dr. R. W.-Y. Sun, Dr. S. C.-F. Kui, Dr. N. Zhu, Prof. Dr. C.-M. Che
Department of Chemistry and Open Laboratory of Chemical Biology of the Institute of Molecular Technology for Drug Discovery and Synthesis
The University of Hong Kong, Pokfulam Road, Hong Kong (China)
Fax: (+852) 2857-1586
E-mail: cmche@hku.hk

Supporting information for this article is available on the WWW under http://www.chemeurj.org/ or from the author.

thesis of [Au(Quinpy)Cl]Cl (HQuinpy = N-(8-quinolyl)pyridine-2-carboxamide) and its derivatives.[2d] These gold(III) compounds are cytotoxic and bind to DNA. In addition, Coronnello, Messori, Fregona, and their co-workers showed recently that gold(III)-induced cytotoxicity may proceed through an induction of apoptosis.[2a,b]

We have reported previously the synthesis and study of a series of gold(III) porphyrins that exhibit potent in vitro and in vivo anticancer properties toward hepatocellular carcinoma and nasopharyngeal carcinoma.[3] As demonstrated by DNA-microarray and proteomic analyses, the gold(III) tetraarylporphyrins upregulated the transcription and translation of a number of apoptosis-related gene and protein expressions. To explore potential medicinal applications for gold(III) compounds, we focused our attention on $[Au_m(C^N^C)_mL]^{n+}$ compounds (HC^N^CH = 2,6-diphenylpyridine, Scheme 1), which were first developed and reported by us in 1998.[5b] We envisioned that the cationic $[Au_m(C^N^C)_mL]^{n+}$ compounds (for $m=1$, $n=1$, L = neutral ligand) would be structurally analogous to the classical metallointercalating $[Pt(terpy)L]^+$ compounds.[6] This class of compounds should be highly robust in solution, because the dianionic nature of the C^N^C ligand would stabilize the electrophilic gold(III), causing its reduction to gold(II) and gold(I) at negative reduction potential. It would also be feasible to make structural modifications to the $[Au_m(C^N^C)_mL]^{n+}$ compounds through ligand-substitution reactions of L, which would be very useful for studying the relationship between structure and cytotoxicity. By using appropriate polydentate ligands, polynuclear gold(III) compounds comprising more than one $[Au(C^N^C)]^+$ moiety ($m=2$ or 3) could be obtained. Furthermore, given the stability of the gold(III)–ligand bond, the $[Au(C^N^C)]^+$ moiety may also serve as a biological carrier through the ligation of cytotoxic agents, such as phosphine ligands.

Here we describe the syntheses of a series of $[Au_m(C^N^C)_mL]^{n+}$ compounds (L = chloride, N-donor, or phosphine ligand). By using [Au(C^N^C)(1-methylimidazole)]$^+$ (**2a**) and $[Au_2(C^N^C)_2(\mu$-1,2-bis(diphenylphosphino)propane$)]^{2+}$ (**3d**) as model compounds, the mode of interaction of $[Au_m(C^N^C)_mL]^{n+}$ with DNA and potential mechanisms for induced cell death are examined.

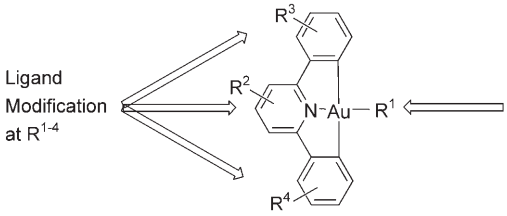

Scheme 1. Possible sites for structural modification of $[Au_m(C^N^C)_mL]^{n+}$.

Results and Discussion

The $[Au_m(C^N^C)_mL]^{n+}$ compounds studied are shown in Scheme 2. The gold(III) compounds, including new compounds **2b**, **2c**, **3d–h**, **4a**, **4b**, and **5a–f**, were prepared according to literature methods and were characterized by ^{1}H NMR and UV-visible spectroscopies, and fast atom-bombardment (FAB) mass spectrometry (see Experimental Sec-

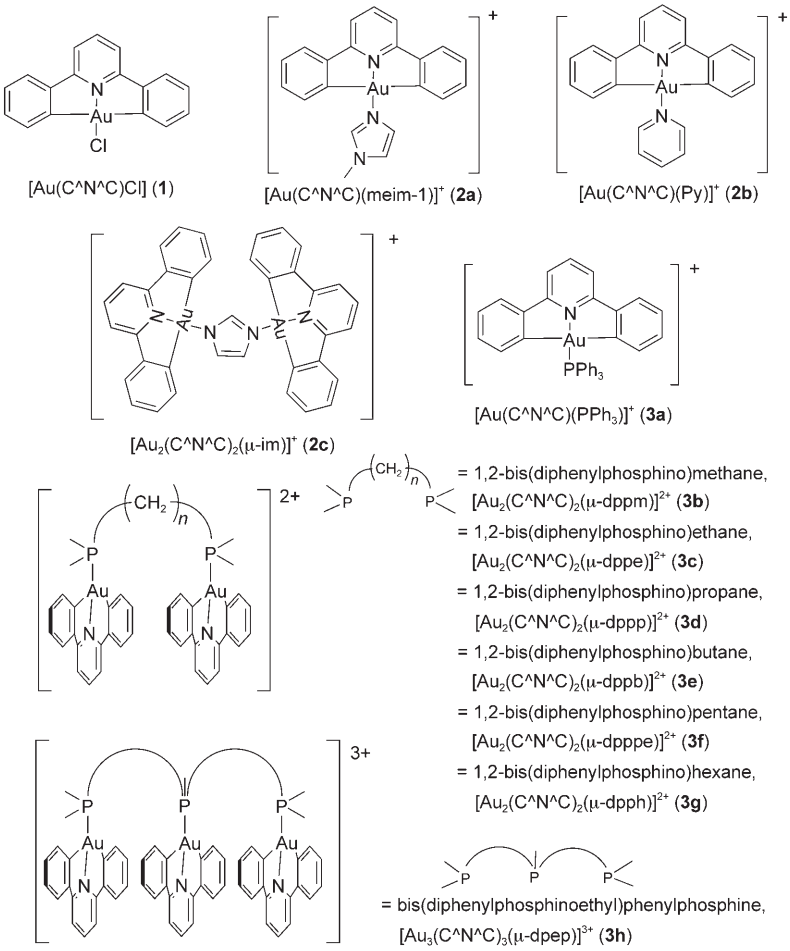

Scheme 2. The gold(III) compounds investigated.

tion).[5,7] Displacement of the chloride group of **1** (R^1 modification, Scheme 1) is achieved by reaction with the appropriate N-donor (**2**) or phosphine (**3**) ligands. By using the bidentate imidazolato (for **2c**), 1,2-bis(diphenylphosphino)C_n (C_n is a saturated hydrocarbon linker with $n=1$–6, for **3b**–**g**), and tridentate bis(diphenylphosphinoethyl)phenylphosphine (for **3h**) ligands, we obtained multinuclear gold(III) compounds containing more than one $[Au(C^N^C)]^+$ moiety. Compounds **4a** and **4b** are structural analogues of **1** and **2a**, respectively, with a phenyl substitution at the R^2 position. Compounds **5a**–**f** are gold(III) compounds containing extended π-conjugated C^N^C motifs (R^3 and R^4 modification on the C^N^C ligand).

X-ray crystallography: The molecular structures of **1** (Figure S1), **2b** (Figure S2), **2c** (Figure 1), **3d** (Figure 2), **3h** (Figure 3), **4a** (Figure S3), **5a** (Figure S4), **5c** (Figure S5), **5d** (Figure S6), **5e** (Figure S7), and **5f** (Figure 4) were established by X-ray crystallography. Crystallographic data-collection parameters and selected bond angles and distances for the gold(III) compounds are summarized in Tables 1 and 2, respectively. The Au–N(pyridyl) distances (1.94–2.06 Å) are comparable to the related distances (1.93–2.14 Å) found in $[Au(terpy)Cl]^{2+}$ (terpy = 2,2′,2″-terpyridine),[4] $[Au(4\text{-}MeOPh\text{-}terpy)Cl]^{2+}$ (4-MeOPh-terpy = 4′-(4-methoxyphenyl)-2,2′,6′,2″-terpyridine),[2i] and $[Au(esal)]^{2+}$ (esal = N-ethylsalicylaldiminate).[2g] The Au–C(phenyl) distances (2.06–2.13 Å) in these structures are comparable to the previously reported $[Au(C^N^C)L]^{n+}$ analogues (2.08–2.16 Å).[5b] The respective angles between the *trans* aryl carbon atoms in all the X-ray crystal structures (156.8–163.8°) deviate significantly from linearity. This is attributed to the phenyl substituents of the 2,6-diphenylpyridine ligand, which evidently restrict the bite angle.

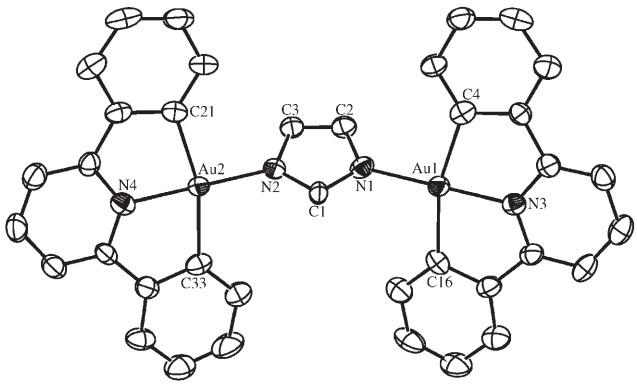

Figure 1. ORTEP drawing of the molecular cation of **2c** made with thermal ellipsoids at the 30% probability level.

The crystal structure of the molecular cation of **2c** (Figure 1) shows two $[Au(C^N^C)]^+$ units that can arrange in C_{2v} symmetry through coordination of the N donors of the bidentate imidazolato ligand to gold(III). In contrast, the dppp ligand of **3d** (dppp = 1,2-bis(diphenylphosphino)propane) can position two $[Au(C^N^C)]^+$ moieties into a face-to-face configuration (Figure 2). This configuration suggests weak intramolecular interactions between the two staggered $[Au(C^N^C)]^+$ units with an interplanar distance of 3.789 Å. However, the intramolecular metal···metal contact of 4.626 Å between Au1···Au2 is beyond the normal range of metal–metal interactions for d^8-metal ions.[8]

Figure 3 depicts the configuration of the molecular cation of the trinuclear gold(III) compounds, with bis(diphenylphosphinoethyl)phenylphosphine (dpep) as the supporting ligand (**3h**). Two of the three planar $[Au(C^N^C)]^+$ moieties of **3h**

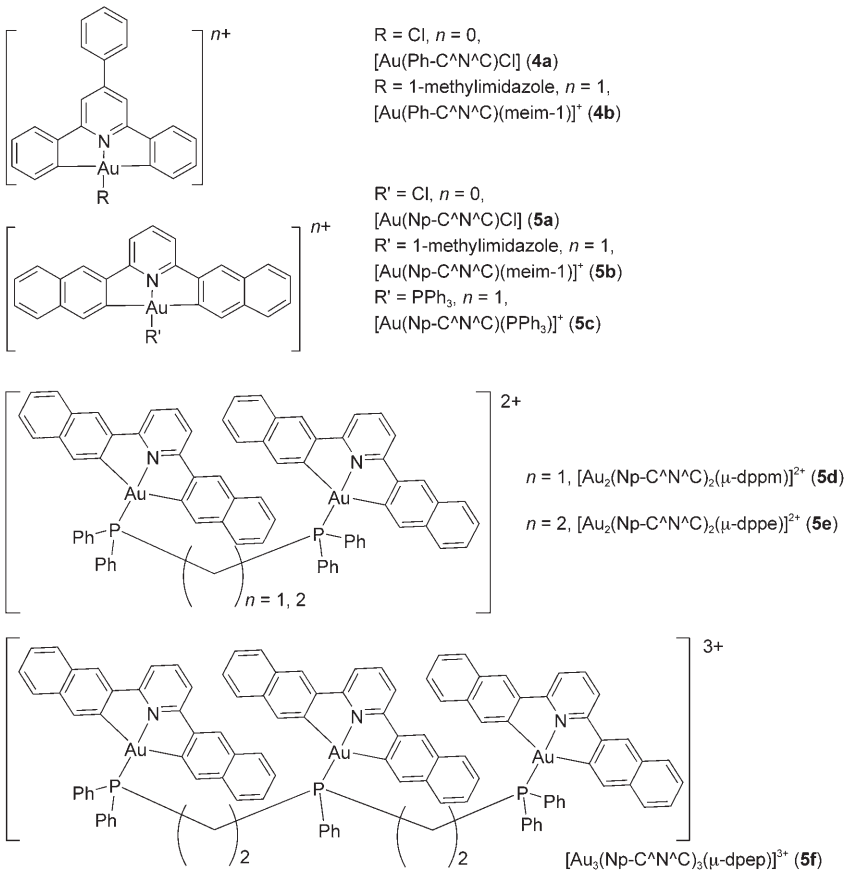

Scheme 2. (Continued)

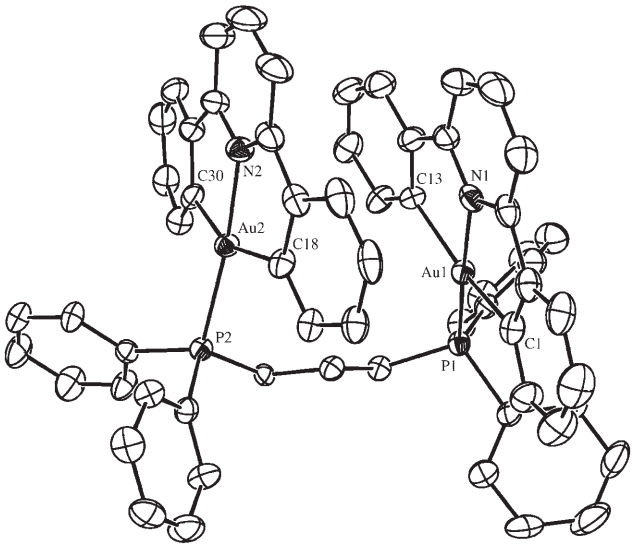

Figure 2. ORTEP drawing of the molecular cation of **3d** made with thermal ellipsoids at the 30% probability level.

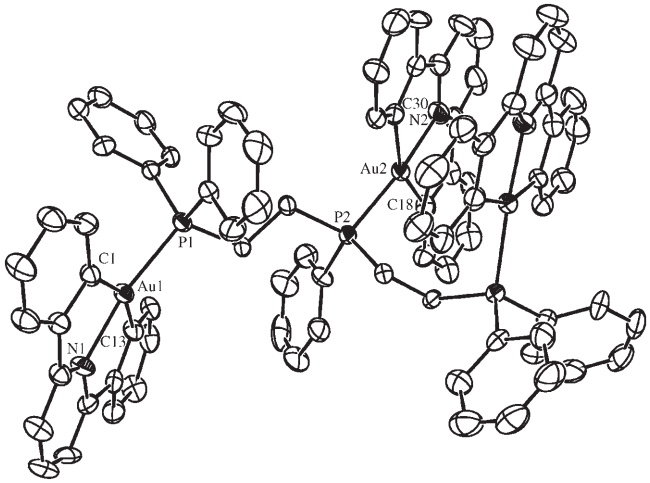

Figure 3. ORTEP drawing of the molecular cation of **3h** made with thermal ellipsoids at the 30% probability level.

are positioned in a face-to-face configuration. Similar to **3d**, there is a weak π···π stacking interaction (3.680 Å) between these two gold(III) moieties. The remaining terminal [Au(C^N^C)]$^+$ moiety sits as a 'flap' on the other side of the molecule along the phosphorus–carbon chain, creating a Au1···Au2···Au3 angle of 99.8°. This angle deviates significantly from linearity, compared with the M···M···M angles of 154–179° found in the reported tethered oligopyridine cyclometalated platinum(II) systems.[8]

The structures of **5a**, **5c**, **5d**, **5e**, and **5f** containing extended π-conjugated C^N^C motifs were also established by X-ray crystallography. The crystal structure of **5a** reveals the presence of π-stacking intermolecular interactions (3.59 Å) (Supporting Information). However, this intermolecular π-stacking distance is larger than that found in **1** (2.84 Å). The interplanar distances between the [Au(Np-C^N^C)]$^+$ (in which Np-C^N^C = 2,6-dinaphthylpyridine) motifs of dinuclear gold(III) compounds **5d** and **5e** are 3.34 and 3.19 Å, respectively, indicative of π-stacking intramolecular interactions for these two gold(III) compounds. Similar to the trinuclear gold(III) compound **3h**, two of the three planar [Au(C^N^C)]$^+$ moieties of **5f** are positioned in a face-to-face configuration, whereas the remaining terminal [Au(C^N^C)]$^+$ moiety sits as a 'flap' on the other side of the molecule along the phosphorus–carbon chain (Figure 4).

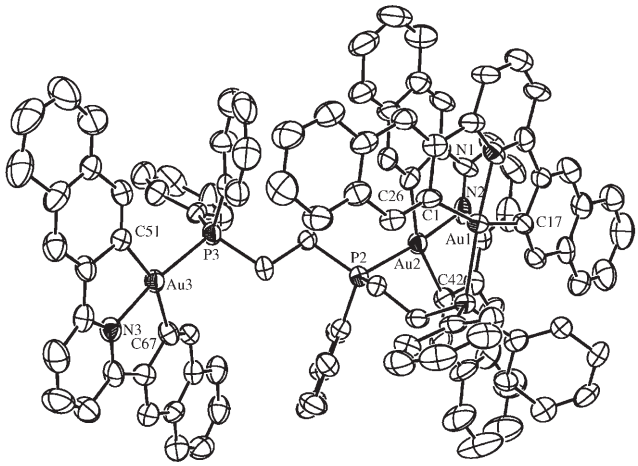

Figure 4. ORTEP drawing of the molecular cation of **5f** made with thermal ellipsoids at the 30% probability level.

Physical properties: Compounds **2a**, **2b**, **3a–h**, **4b**, and **5b–f** are slightly soluble in water, with solubilities of ~0.5 mg mL^{-1}. Unlike the neutral phosphine ligands themselves, which are insoluble in water and poorly soluble in dimethyl sulfoxide (DMSO), the gold(III) compounds **3a–h** possess positive charge(s), giving them better solubility in polar solvents. The neutral compounds **1**, **4a**, and **5a**, and the cationic dinuclear gold(III) compound **2c** are insoluble in water, but could be dissolved in DMSO and DMF at ~1 mg mL^{-1}. All these gold(III) compounds exhibit a vibronic-structure absorption band with peak maxima at 304–318 nm in DMSO. As reported previously, these absorptions are attributed to a metal-perturbed intraligand (IL) π–π* transition within the C^N^C ligand.[5] At a concentration of 50 μM, all compounds exhibited excellent stability in organic solvents, as no significant UV-visible spectral changes were observed over a 24-h period at room temperature. Electrochemical properties of the gold(III) compounds in DMF were studied by cyclic voltammetry. Compared to $KAuCl_4$ [$E^o_{\text{gold(III)}\rightarrow\text{gold(I)}} = -0.4$ V], the substantially more-cathodic potentials of −1.43 to −1.83 V versus $Cp_2Fe^{+/0}$ required for the gold(III) reduction in all the gold(III) compounds is consistent with stabilization of gold(III) by the dianionic C^N^C ligand (Table S1). Thus, it is not surprising that these gold(III) compounds are not reduced easily under physiological conditions. Treatment of the gold(III) compounds, such as **2a**, with glutathione (GSH, 2 mM) in Tris-buffered saline

Table 1. Crystal data and structure refinement for **1**, **2b**-(ClO_4), **2c**-(ClO_4)·C_3H_7NO, **3d**-$(CF_3SO_3)_2$·4 CH_3CN, **3h**-$(CF_3SO_3)_3$·CH_3CN·H_2O, **4a**·CH_3OH, **5a**, **5c**-(CF_3SO_3)·$CHCl_3$, **5d**-$(CF_3SO_3)_2$·H_2O, **5e**-$(CF_3SO_3)_2$·2 Et_2O, and **5f**-$(CF_3SO_3)_3$·6 $CHCl_3$·H_2O.

	1	**2b**-(ClO_4)	**2c**-(ClO_4)·C_3H_7NO	**3d**-$(CF_3SO_3)_2$·4 CH_3CN	**3h**-$(CF_3SO_3)_3$·CH_3CN·H_2O	**4a**·CH_3OH
formula	$C_{17}H_{11}ClNAu$	$C_{22}H_{16}ClN_2O_4Au$	$C_{37}H_{25}ClN_4O_4Au_2$·C_3H_7NO	$C_{63}H_{48}F_6N_2O_6P_2S_2Au_2$·$C_8H_{12}N_4$	$C_{88}H_{66}F_9N_3O_9P_3S_3Au_3$·$C_2H_3N$·$H_2O$	$C_{23}H_{15}NClAu$·CH_4O
M_r	461.68	604.78	1092.09	1727.24	2319.48	569.80
cryst. system	monoclinic	triclinic	monoclinic	monoclinic	triclinic	orthorhombic
space group	*C*2/*c*	$P\bar{1}$	$P2_1/n$	$P2_1/c$	$P\bar{1}$	*Fddd*
a [Å]	10.595(2)	8.911(2)	13.453(3)	21.760(5)	13.082(3)	11.820(2)
b [Å]	13.995(3)	10.632(2)	18.847(4)	17.740(4)	14.668(3)	15.064(3)
c [Å]	9.293(2)	12.072(2)	15.143(3)	17.959(4)	25.067(5)	46.414(9)
α [°]	90.00	106.60(3)	90.00	90.00	96.84(3)	90.00
β [°]	101.26(3)	93.25(3)	109.85(3)	90.17(3)	92.35(3)	90.00
γ [°]	90.00	112.84(3)	90.00	90.00	109.43(3)	90.00
V [Å^3]	1351.4(5)	991.8(3)	3611.4(13)	6933(3)	4487.1(16)	8264.0(3)
Z	4	2	4	4	2	16
F(000)	864	580	2088	3400	2256	4352
ρ_{calcd} [Mg m^{-3}]	2.269	2.025	2.009	1.655	1.715	1.825
μ [mm^{-1}]	11.070	7.585	8.243	4.406	5.093	7.263
index ranges	$-12 \le h \le 12$	$-9 \le h \le 9$	$-16 \le h \le 16$	$-26 \le h \le 26$	$-15 \le h \le 15$	$-14 \le h \le 9$
	$-16 \le k \le 16$	$-12 \le k \le 12$	$-22 \le k \le 22$	$-21 \le k \le 21$	$-17 \le k \le 17$	$-11 \le k \le 18$
	$-10 \le l \le 9$	$-14 \le l \le 14$	$-18 \le l \le 18$	$-21 \le l \le 21$	$-30 \le l \le 29$	$-53 \le l \le 53$
reflns collected	4595	7053	25187	50377	31154	6720
independent reflns	1162	3361	6389	12724	15316	1714
data/restraints/parameters	1162/0/93	3361/58/267	6389/0/478	12724/0/850	15316/93/1059	1714/0/117
final *R* indices [$I > 2\sigma(I)$]	$R1 = 0.033$	$R1 = 0.042$	$R1 = 0.043$	$R1 = 0.037$	$R1 = 0.049$	$R1 = 0.041$
	$wR2 = 0.079$	$wR2 = 0.096$	$wR2 = 0.102$	$wR2 = 0.076$	$wR2 = 0.124$	$wR2 = 0.099$
goodness-of-fit on F^2	1.162	0.964	0.895	0.829	0.918	0.962
largest diff. peak/hole [eÅ^{-3}]	0.740/−1.803	2.083/−2.082	1.534/−2.498	1.300/−1.444	1.405/−2.058	1.225/−1.915

	5a	**5c**-(CF_3SO_3)·$CHCl_3$	**5d**-$(CF_3SO_3)_2$·H_2O	**5e**-$(CF_3SO_3)_2$·2 Et_2O	**5f**-$(CF_3SO_3)_3$·6 $CHCl_3$·H_2O
formula	$C_{25}H_{15}ClNAu$	$C_{44}H_{29}F_3NO_3PSAu$·$CHCl_3$	$C_{77}H_{52}F_6N_2O_6P_2S_2Au_2$·$H_2O$	$C_{78}H_{54}F_6N_2O_6P_2S_2Au_2$·$C_8H_{20}O_2$	$C_{112}H_{78}F_9N_3O_9P_3S_3Au_3$·$C_6H_8Cl_{18}O$
M_r	561.80	1056.05	1753.21	1897.46	3294.99
cryst. system	orthorhombic	triclinic	monoclinic	monoclinic	triclinic
space group	*Pbca*	$P\bar{1}$	$P2_1/c$	*C*2/*c*	$P\bar{1}$
a [Å]	15.303(3)	9.662(2)	24.777(5)	40.037(8)	16.044(3)
b [Å]	9.699(2)	13.853(3)	14.959(3)	14.516(3)	17.338(4)
c [Å]	25.666(5)	15.567(3)	18.165(4)	42.375(9)	25.463(5)
α [°]	90.00	93.08(3)	90.00	90.00	97.52(3)
β [°]	90.00	90.22(3)	100.78(3)	104.76(3)	102.51(3)
γ [°]	90.00	101.28(3)	90.00	90.00	109.12(3)
V [Å^3]	3809.4(13)	2040.2(7)	6614(2)	23815(9)	6375(2)
Z	8	2	4	12	2
F(000)	2144	1038	3440	11304	3224
ρ_{calcd} [Mg m^{-3}]	1.959	1.719	1.761	1.588	1.717
μ [mm^{-1}]	7.874	3.949	4.619	3.856	3.978
index ranges	$-15 \le h \le 15$	$-11 \le h \le 8$	$-29 \le h \le 29$	$-45 \le h \le 45$	$-17 \le h \le 17$
	$-9 \le k \le 9$	$-16 \le k \le 15$	$-18 \le k \le 18$	$-17 \le k \le 17$	$-20 \le k \le 20$
	$-29 \le l \le 29$	$-18 \le l \le 18$	$-21 \le l \le 21$	$-50 \le l \le 50$	$-29 \le l \le 30$
reflns collected	11847	10158	45673	58958	38662
independent reflns	2198	6662	11809	19276	19309
data/restraints/parameters	2198/0/63	6662/22/537	11809/19/863	19276/275/1290	19309/297/1328
final *R* indices [$I > 2\sigma(I)$]	$R1 = 0.062$	$R1 = 0.037$	$R1 = 0.035$	$R1 = 0.051$	$R1 = 0.065$
	$wR2 = 0.187$	$wR2 = 0.086$	$wR2 = 0.077$	$wR2 = 0.122$	$wR2 = 0.171$
goodness-of-fit on F^2	0.935	0.986	0.775	0.852	0.919
largest diff. peak/hole [eÅ^{-3}]	0.998/−1.382	1.074/−1.492	1.208/−0.925	2.515/−0.904	1.285/−1.491

(TBS)/DMSO (9:1) solution caused no significant UV-visible spectral changes over a 24-h period (Figure S8). ESI-MS analysis of the solution revealed the presence of only the molecular ion of $[Au(C^N^C)(meim\text{-}1)]^+$ (meim-1 = 1-methylimidazole), ($m/z = 508$, Figure S9) with no evidence of demetalation. These findings indicate that **2a** did not undergo demetalation upon treatment with GSH. In addition, there were no changes in UV-visible, ^{31}P NMR, or ^1H NMR spectra (Figure S10) observed for **3d** (as an example of a phosphine-containing gold(III) compound) upon standing in DMSO or TBS for 24 h. This observation demonstrates that these gold(III) compounds are stable in solution.

Table 2. Selected bond lengths [Å] and angles [°] for **1**, **2b**-(ClO_4), **2c**-(ClO_4)·C_3H_7NO, **3d**-$(CF_3SO_3)_2$·4CH_3CN, **3h**-$(CF_3SO_3)_3$·CH_3CN·H_2O, **4a**·CH_3OH, **5a**, **5c**-(CF_3SO_3)·$CHCl_3$, **5d**-$(CF_3SO_3)_2$·H_2O, **5e**-$(CF_3SO_3)_2$·2Et_2O, and **5f**-$(CF_3SO_3)_3$·6$CHCl_3$·H_2O.

1[a]		**2b**-(ClO_4)	
Au1−N1	1.984(8)	Au1−N1	1.980(8)
Au1−C1	2.094(7)	Au1−C1	2.073(9)
Au1−C1#1	2.094(7)	Au1−C13	2.081(9)
Au1−Cl1	2.282(2)	Au1−N2	2.043(7)
N1-Au1-C1	81.7(2)	N1-Au1-C1	82.6(4)
N1-Au1-C1#1	81.7(2)	N1-Au1-C13	81.2(4)
C1-Au1-C1#1	163.3(4)	C1-Au1-C13	163.8(4)
N1-Au1-Cl1	180.0(1)	N1-Au1-N2	178.2(3)
C1-Au1-Cl1	98.3(2)	C1-Au1-N2	98.8(3)
C1#1-Au1-Cl1	98.3(2)	C13-Au1-N2	97.4(3)

2c-(ClO_4)·C_3H_7NO		**3d**-$(CF_3SO_3)_2$·4CH_3CN		**3h**-$(CF_3SO_3)_3$·CH_3CN·H_2O			
Au1−N3	1.953(8)	Au1−N1	2.028(5)	Au1−N1	2.047(8)	C18-Au2-C30	159.9(4)
Au1−C4	2.085(9)	Au1−C1	2.119(6)	Au1−C1	2.092(9)	N2-Au2-P2	173.1(3)
Au1−C16	2.077(10)	Au1−C13	2.100(6)	Au1−C13	2.098(8)	C18-Au2-P2	101.3(3)
Au1−N1	2.016(8)	Au1−P1	2.296(15)	Au1−P1	2.274(3)	C30-Au2-P2	98.6(3)
Au2−N4	1.957(8)	Au2−N2	2.015(5)	Au2−N2	2.042(9)	N3-Au3-C35	81.3(4)
Au2−C21	2.080(9)	Au2−C18	2.117(6)	Au2−C18	2.110(10)	N3-Au3-C47	78.6(4)
Au2−C33	2.090(10)	Au2−C30	2.105(6)	Au2−C30	2.110(8)	C35-Au3-C47	159.4(4)
Au2−N2	1.991(9)	Au2−P2	2.283(16)	Au2−P2	2.288(3)	N3-Au3-P3	176.0(3)
				Au3−N3	2.032(8)	C35-Au3-P3	99.2(3)
N3-Au1-C4	81.8(4)	N1-Au1-C1	80.2(2)	Au3−C35	2.087(12)	C47-Au3-P3	101.2(3)
N3-Au1-C16	81.9(4)	N1-Au1-C13	80.3(2)	Au3−C47	2.095(11)		
C4-Au1-C16	163.6(4)	C1-Au1-C13	159.9(2)	Au3−P3	2.288(3)		
N3-Au1-N1	178.5(3)	N1-Au1-P1	174.41(15)				
C4-Au1-N1	97.5(4)	C1-Au1-P1	103.17(17)	N1-Au1-C1	80.4(3)		
C16-Au1-N1	98.9(4)	C13-Au1-P1	96.65(17)	N1-Au1-C13	80.5(4)		
N4-Au2-C21	82.3(4)	N2-Au2-C18	80.6(2)	C1-Au1-C13	159.8(4)		
N4-Au2-C33	80.9(4)	N2-Au2-C30	80.2(2)	N1-Au1-P1	169.3(2)		
C21-Au2-C33	163.2(5)	C18-Au2-C30	159.4(3)	C1-Au1-P1	100.7(3)		
N4-Au2-N2	179.5(3)	N2-Au2-P2	174.03(15)	C13-Au1-P1	99.3(3)		
C21-Au2-N2	97.4(4)	C18-Au2-P2	102.15(18)	N2-Au2-C18	78.8(4)		
C33-Au2-N2	99.4(4)	C30-Au2-P2	97.67(18)	N2-Au2-C30	81.8(4)		

4a·CH_3OH[b]		**5a**		**5c**-(CF_3SO_3)·$CHCl_3$	
Au1−N1	1.979(8)	Au1−N1	1.941(11)	Au1−N1	2.040(4)
Au1−C1	2.111(16)	Au1−C2	2.063(9)	Au1−C1	2.088(6)
Au1−C1#2	2.111(16)	Au1−C18	2.086(7)	Au1−C17	2.096(5)
Au1−Cl1	2.287(3)	Au1−Cl1	2.269(6)	Au1−P1	2.297(14)
N1-Au1-C1	78.4(4)	N1-Au1-C2	81.1(6)	N1-Au1-C1	80.95(19)
N1-Au1-C1#2	78.4(4)	N1-Au1-C18	82.4(5)	N1-Au1-C17	80.26(19)
C1-Au1-C1#2	156.8(8)	C2-Au1-C18	163.5(5)	C1-Au1-C17	161.2(2)
N1-Au1-Cl1	180.0(0)	N1-Au1-Cl1	179.7(4)	N1-Au1-P1	176.33(12)
C1-Au1-Cl1	101.6(4)	C2-Au1-Cl1	98.7(4)	C1-Au1-P1	95.38(15)
C1#2-Au1-Cl1	101.6(4)	C18-Au1-Cl1	97.8(4)	C17-Au1-P1	103.41(15)

5d-$(CF_3SO_3)_2$·H_2O		**5e**-$(CF_3SO_3)_2$·2Et_2O		**5f**-$(CF_3SO_3)_3$·6$CHCl_3$·H_2O			
Au1−N1	2.060(5)	Au1−N1	2.029(8)	Au1−N1	2.042(11)	C26-Au2-C42	160.7(5)
Au1−C1	2.126(6)	Au1−C1	2.088(9)	Au1−C1	2.116(12)	N2-Au2-P2	172.7(3)
Au1−C17	2.127(6)	Au1−C17	2.093(10)	Au1−C17	2.079(13)	C26-Au2-P2	97.1(4)
Au1−P1	2.303(19)	Au1−P1	2.287(2)	Au1−P1	2.293(4)	C42-Au2-P2	101.7(4)
Au2−N2	2.044(5)	Au2−N2	2.033(9)	Au2−N2	2.059(11)	N3-Au3-C51	80.9(5)
Au2−C42	2.114(6)	Au2−C42	2.080(13)	Au2−C42	2.115(14)	C51-Au3-C67	162.5(6)
Au2−C26	2.114(6)	Au2−C26	2.129(10)	Au2−C26	2.070(15)	N3-Au3-C67	82.4(5)
Au2−P2	2.297(18)	Au2−P2	2.292(3)	Au2−P2	2.288(3)	N3-Au3-P3	171.1(3)
				Au3−N3	2.016(11)	C51-Au3-P3	101.9(4)
N1-Au1-C1	80.0(2)	N1-Au1-C1	80.1(4)	Au3−C51	2.100(13)	C67-Au3-P3	95.4(4)
N1-Au1-C17	79.4(2)	N1-Au1-C17	80.7(4)	Au3−C67	2.094(15)		
C1-Au1-C17	159.4(3)	C1-Au1-C17	160.6(4)	Au3−P3	2.289(4)		
N1-Au1-P1	176.94(14)	N1-Au1-P1	176.6(2)				
C1-Au1-P1	102.7(2)	C1-Au1-P1	100.7(3)	N1-Au1-C1	80.9(5)		
C17-Au1-P1	97.9(2)	C17-Au1-P1	98.6(3)	N1-Au1-C17	80.3(5)		
N2-Au2-C26	80.6(2)	N2-Au2-C26	80.6(4)	C1-Au1-C17	160.1(5)		

Table 2. (Continued)

5d-$(CF_3SO_3)_2\cdot H_2O$		**5e**-$(CF_3SO_3)_2\cdot 2Et_2O$		**5f**-$(CF_3SO_3)_3\cdot 6CHCl_3\cdot H_2O$	
N2-Au2-C42	80.2(2)	N2-Au2-C42	80.3(5)	N1-Au1-P1	174.9(3)
C26-Au2-C42	160.7(3)	C26-Au2-C42	160.4(5)	C1-Au1-P1	99.3(4)
N2-Au2-P2	175.93(13)	N2-Au2-P2	175.9(3)	C17-Au1-P1	100.0(4)
C26-Au2-P2	95.60(19)	C26-Au2-P2	97.7(3)	N2-Au2-C26	79.8(6)
C42-Au2-P2	103.58(19)	C42-Au2-P2	101.5(4)	N2-Au2-C42	81.9(5)

[a] Symmetry operation #1: $-x+1, y, -z+0.5$ [b] Symmetry operation #2: $-x+0.75, -y+0.75, z$.

Cytotoxicity of the $[Au_m(C\hat{}N\hat{}C)_mL]^{n+}$ compounds containing nontoxic N-donor auxiliary ligands: The cytotoxicities of the gold(III) compounds toward several human cancer cell lines, including nasopharyngeal carcinoma (SUNE1, and its cisplatin variant CNE1), hepatocellular carcinoma (HepG2), and cervical epithelioid carcinoma (HeLa) were determined by using a well-established MTT assay.[9] The results are listed in Table 3. Modification of **1** at position R^1 (Scheme 1) by using various N-donor ligands gave compounds **2a**–**c**, the IC_{50} values of which spanned the range 1.5–84 μM. The cytotoxicities of some of these compounds were found to be similar to that of cisplatin (1.0–11 μM) and the classical metallointercalator [Pt(terpy)Cl]Cl (11–23 μM). In contrast to similar reported compounds, these gold(III) compounds possess slightly lower cytotoxic activities than the gold(III) tetraarylporphyrins[3] and $[Au(terpy)Cl]Cl_2$,[2f] but exhibit cytotoxicities similar to other classes of gold(III) cyclometalated compounds, such as $[Au^{III}(bipy^c\text{-}H)(OH)][PF_6]$ ($bipy^c$-H = deprotonated 1,1-dimethylbenzyl-2,2-bipyridine)[2e] and $[Au^{III}(dmamp)Cl_2]$ (dmamp = 2-(dimethylaminomethyl)phenyl).[2h] As a control, the cytotoxicities of the metal-free N-donor ligands (1-methylimidazole, pyridine, and imidazole) were also examined. Their IC_{50} values were found to be >100 μM (data not shown), suggesting that these ligands are relatively nontoxic. Because structural modification at R^1 by using these nontoxic N-donor ligands has little influence on cytotoxicity, it is, therefore, the $[Au(C\hat{}N\hat{}C)]^+$ moiety that is instrumental for the observed cytotoxicity.

Cisplatin chemotherapy is currently the last-line treatment for several types of cancer, including nasopharyngeal carcinoma (NPC). However, resistance to cisplatin is frequently encountered.[10] Thus, new anticancer agents that are active against cisplatin-resistant cell lines are required. As shown in Table 3, the gold(III) compounds are equally cytotoxic toward the cisplatin-sensitive and -resistant NPC (SUNE1 and CNE1, respectively). The resistance factor, IC_{50} (CNE1/SUNE1), for cisplatin is 3.3, whereas the corresponding values for the gold(III) compounds are close to unity (Table 3). The lack of cross resistance suggests that the gold(III) compounds and cisplatin may induce cytotoxicity through different mechanisms, or the gold(III) compounds may bypass the cellular-sequestration mechanism for cytotoxic agents (e.g., they are stable in elevated levels of GSH).

We also examined the cytotoxicity of the gold(III) compounds with R^2 (**4**) or R^3 and R^4 (**5**) modifications (see Scheme 1). Both **4b** ($IC_{50(SUNE1)}=2.4$ μM; $IC_{50(CNE1)}=2.3$ μM) and **5b** ($IC_{50(SUNE1)}=7.8$ μM; $IC_{50(CNE1)}=8.5$ μM) with 1-methylimidazole as auxiliary ligands exhibit cytotoxic activities similar to that of **2a** (c.f., $IC_{50(SUNE1)}=12$ μM; $IC_{50(CNE1)}=6.7$ μM). It appears that extension of the planar C^N^C ligand by modifying the R^2–R^4 positions does not play an important role in the overall $[Au(C\hat{}N\hat{}C)]^+$ cytotoxicity.

Table 3. Cytotoxicities (IC_{50}, 72 h) of the gold(III) compounds toward selected human cancer cell lines.

Compound	IC_{50} [μM] HeLa[b]	HepG2[b]	SUNE1[b]	CNE1[b]	IC_{50} ratio (CNE1/SUNE1)
1	3.4±0.6	17±2	4.0±0.5	3.1±0.4	0.78
2a	8.0±0.5	35±5	12±1.3	6.7±1.5	0.56
2b	8.2±0.4	84±12	4.0±0.4	2.6±0.4	0.65
2c	3.0±0.2	54±6	2.1±0.3	1.5±0.3	0.71
3a	n.d.[a]	n.d.[a]	17±2	11±2	0.65
3b	0.81±0.08	n.d.[a]	0.92±0.12	1.2±0.2	1.3
3c	0.14±0.03	0.32±0.08	0.25±0.03	0.40±0.06	1.6
3d	0.043±0.006	0.21±0.09	0.055±0.007	0.091±0.012	1.7
3e	2.4±0.2	n.d.[a]	1.5±0.2	2.2±0.3	1.5
3f	1.5±0.3	n.d.[a]	1.6±0.3	2.5±0.3	1.6
3g	3.2±0.4	n.d.[a]	4.3±0.9	3.2±0.5	0.74
3h	0.93±0.09	3.8±0.6	0.26±0.03	0.40±0.05	1.5
4b	4.6±0.8	13±2	2.4±0.4	2.3±0.6	0.96
5b	17±3	n.d.[a]	7.8±1.2	8.5±0.9	1.1
[Pt(terpy)Cl]Cl	14±2	23±3	11±3	13±2	1.2
cisplatin	11±1	1.6±0.2	1.0±0.1	3.3±0.5	3.3

[a] n.d. = not determined. [b] HeLa = human cervical epithelioid carcinoma; HepG2 = human hepatocellular carcinoma; SUNE1 = human nasopharyngeal carcinoma (cisplatin sensitive); CNE1 = human nasopharyngeal carcinoma (cisplatin resistant).

The $[Au(C\hat{}N\hat{}C)]^+$ moiety serves as a carrier of cytotoxic phosphine compounds: As reviewed by Sadler and Berners-Price in 1987,[11b] phosphine-containing compounds are well-known potential anticancer agents.[11] However, their instability under physiological conditions (e.g., formation of phosphine oxide) and nonspecific binding affinities toward various biomolecules have hindered their clinical development as anticancer agents. In this work, we found that the [Au-

$(C^N^C)]^+$ moiety may be used as a carrier for phosphino compounds.

A number of structurally distinct gold(III)-phosphino compounds (**3b–g**) were synthesized and assayed for cytotoxic activities toward several cancer cell lines (see Table 3). All these gold(III) compounds were found to be highly cytotoxic, with IC_{50} values between 0.04 and 4.3 μM. Among the gold(III)-1,2-bis(diphenylphosphino)C_n analogues (C_n is a saturated hydrocarbon linker with $n=1$–6), 1,2-bis(diphenylphosphino)propane (dppp) tethered by two $[Au(C^N^C)]^+$ units (**3d**) was found to be the most cytotoxic agent, with IC_{50} values toward SUNE1 and HeLa cells of 0.04 and 0.05 μM, respectively. In contrast, shortening ($n=1$ or 2) or lengthening ($n=4$, 5, or 6) the hydrocarbon linker reduced the cytotoxicity, with IC_{50} values increasing by at least one order of magnitude (Figure 5).

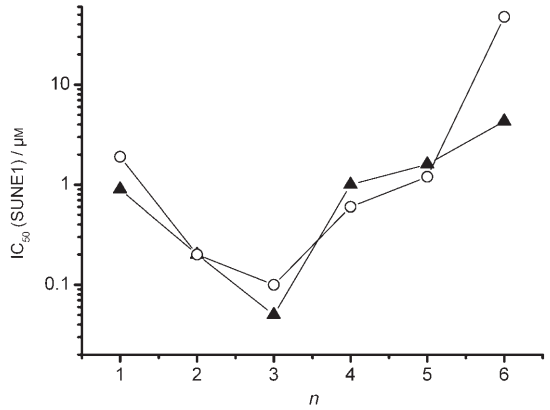

Figure 5. Correlation between the IC_{50} values toward SUNE1 cells and C_n (C_n is the saturated hydrocarbon linker with $n=1$–6) for the metal-free 1,2-bis(diphenylphosphino)C_n (○) or gold(III)-containing (▲) compounds.

As depicted in Figure 5 and Table 4, the IC_{50} values for the metal-free 1,2-bis(diphenylphosphino)C_n compounds follow a trend similar to that of the corresponding gold(III) cyclometalated compounds (**3b–g**), with dppp and $[Au_2(C^N^C)_2(\mu\text{-dppp})]^{2+}$ (**3d**) being the most cytotoxic metal-free and metalated agents, respectively. It appears that the cytotoxicities of these gold(III) compounds are phosphine-mediated. By conducting cellular-uptake experiments, we found that the cytotoxicities of the phosphine-containing compounds are not mediated solely by the $[Au(C^N^C)]^+$ unit. SUNE1 cells treated separately with **3b–g** (50 μM, 2-h incubation) were subjected to inductively coupled plasma mass spectrometry (ICP-MS) for Au analysis. As shown in Table 4, the treated cells showed similar cellular absorptions of Au, spanning the range of 1.18–3.81 ng/cell. Clearly, these cellular absorptions of Au do not follow the trend of IC_{50} values for gold(III)-1,2-bis(diphenylphosphino)C_n, which reveals the presence of non-gold-mediated cytotoxicity.

Table 4. Cytotoxicities ($IC_{50(SUNE1)}$, 72 h) and cellular-uptake data for the phosphine-containing compounds.

Compound	IC_{50} [μM]	IC_{50} of metal-free ligand [μM]	Cellular uptake of gold [ng cell^{-1}]
3b	0.92 ± 0.12	1.9 ± 0.3	2.56 ± 0.02
3c	0.25 ± 0.03	0.22 ± 0.05	3.81 ± 0.13
3d	0.055 ± 0.007	0.13 ± 0.03	2.04 ± 0.32
3e	1.5 ± 0.2	0.62 ± 0.12	1.18 ± 0.27
3f	1.6 ± 0.3	1.2 ± 0.2	2.13 ± 0.59
3g	4.3 ± 0.9	38 ± 6	1.44 ± 0.07

As mentioned above, the stabilities and aqueous solubilities of the phosphine ligands were improved by their ligation to the $[Au(C^N^C)]^+$ moieties. Taking its inherent cytotoxicity into consideration, our results show that the $[Au(C^N^C)]^+$ moiety can serve as a pendant carrier of phosphine ligands in biological systems.

Unlike the phosphine-containing gold(III) compounds, $[Au(C^N^C)]^+$ moieties with nontoxic N-donor auxiliary ligands (**2**) possess instrumental $[Au(C^N^C)]^+$ cytotoxicity. By using $[Au(C^N^C)(1\text{-methylimidazole})]^+$ (**2a**) as a model compound, possible mechanism(s) for its cytotoxic action were delineated.

Induction of apoptosis: Because cancer is characterized by uncontrolled cellular proliferation, there is a considerable interest in chemotherapeutic-induced apoptosis.[12] By using fluorescein-labeled annexin V (AV–FITC) and propidium iodide (PI), the apoptosis-inducing properties of **2a** in SUNE1 cells were examined by performing flow cytometry. Upon treatment with **2a** (60 μM) for 72 h (Figure 6), 30.9% of SUNE1 cells were found to be in early apoptotic state. The apoptosis-inducing properties of **2a** at a lower dose

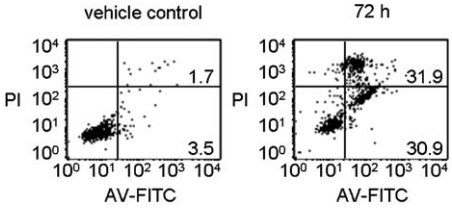

Figure 6. Flow-cytometric study of **2a**-induced apoptosis of SUNE1 cells. Plots show the occurrence of events as functions of fluorescence intensities of PI (*y*-axis) and AV–FITC (*x*-axis). Panels show the fluorescent data for the untreated (vehicle control, left) and **2a**-treated (60 μM, right) cells, corresponding to 3.5 and 30.9% early-stage apoptosis, respectively (bottom right quadrants), after 72-h incubation.

(12 μM for 72 h) were also examined. We found that ~90% of viable cells were unstained by both AV–FITC and PI. The percentage of cell death in cells treated with **2a** at 12 μM (the IC_{50} value) did not reach 50%. According to the propagation profiles (formazan absorbance A_{550nm} vs incubation time, Figure 7) of the treated SUNE1 cells, there is a trend of cellular-growth inhibition in the presence of 12 μM **2a**. Taken together with the flow-cytometric results, these observations suggest that **2a** appears to inhibit cancer-cell proliferation at 12 μM and induce apoptosis at higher doses (i.e., at 60 μM).

DNA binding: DNA is a major target for anticancer drugs,[13] and the binding of gold(III) compounds to DNA has been studied extensively.[2,3] The binding affinities of the

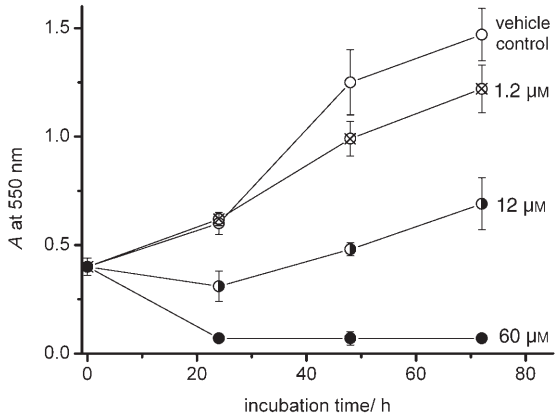

Figure 7. Propagation profiles (formazan absorbance vs incubation time) of SUNE1 cells in the presence (1.2, 12, and 60 μM) and absence of **2a**.

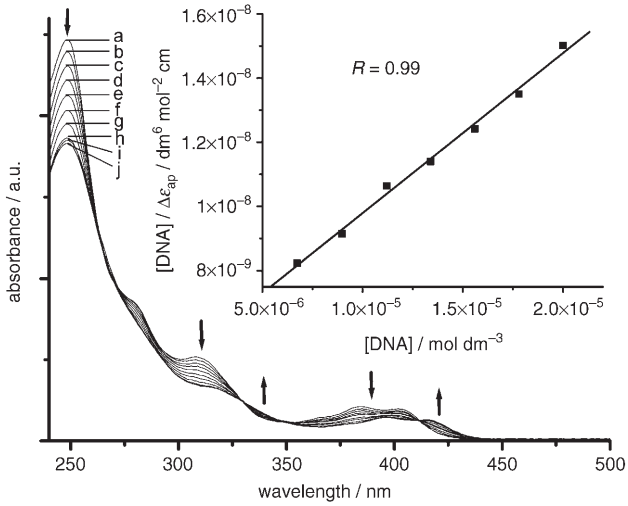

Figure 8. Electronic spectra of **2a** (25 μM) in TBS/DMSO (9:1) with increasing [calf-thymus DNA] at 298 K. [ctDNA]/[**2a**] = 0 (a), 0.1 (b), 0.2 (c), 0.3 (d), 0.4 (e), 0.5 (f), 0.6 (g), 0.7 (h), 0.8 (i), and 0.9 (j). Inset: plot of [ctDNA]/$\Delta\varepsilon_{ap}$ vs [ctDNA].

N-donor-containing **2a**, and the phosphino-containing compounds **3a** and **3d** to calf-thymus DNA (ctDNA) were estimated by measuring changes in DNA melting temperature (T_m).[14] Melting curves for the ctDNA (plots of A_{260} vs temperature) in the absence and presence of **2a**, **3a**, or **3d** are shown in Figure S11. There was a significant increase in the melting point of the ctDNA from 82 to 98.5 °C (i.e., enhanced stabilization) in the presence of **2a**, indicative of binding to ctDNA. However, the DNA melting temperatures increased only slightly, from 82 to 82.9 or 83.5 °C in the presence of **3a** and **3d**, respectively. This suggests that the two gold(III) compounds containing phosphine ligands interact only weakly with ctDNA. It is likely that the sterically demanding phosphino groups impede the interaction of the [Au(C^N^C)] moiety with ctDNA.

We also examined the DNA interactions of three gold(III) complexes by means of UV-visible absorption titration. Isosbestic spectral changes and hyperchromicity (~47%) were observed for the intraligand transitions (~380–420 nm) of the [Au(C^N^C)] moiety upon addition of ctDNA (0–20 μM) to a solution of **2a** (Figure 8). The binding constant (K_b) of **2a** toward ctDNA was determined from the plot of [ctDNA]/$\Delta\varepsilon_{ap}$ versus [ctDNA][15] to be $(4.5\pm0.6)\times10^5$ dm^3 mol^{-1} at 298 K, which is comparable to that of the $[Pt(terpy)L]^+$ compounds.[16] To determine possible DNA-sequence selectivity, binding properties of **2a** to the synthetic oligonucleotides poly(dA–dT)$_2$ (Figure S12) and poly(dG–dC)$_2$ (Figure S13) were also examined. Absorption titration revealed that **2a** exhibits similar binding affinities toward these two oligonucleotides, with K_b of $(2.1\pm0.7)\times10^5$ and $(5.1\pm1.0)\times10^5$ dm^3 mol^{-1} for poly(dA–dT)$_2$ and poly(dG–dC)$_2$ at 298 K, respectively. The binding affinities of the gold(III) compounds containing phosphine ligands (triphenylphosphine, **3a**; 1,2-bis(diphenylphosphino)propane, **3d**) toward ctDNA were also determined. Linear plots (R = 0.99) revealed K_b values of $(2.1\pm0.7)\times10^4$ dm^3 mol^{-1} for **3a** (Figure S14) and $(7.1\pm0.7)\times10^3$ dm^3 mol^{-1} for **3d** (Figure S15), ~30- and ~100-fold lower than those of **2a**, respectively.

Compound 2a intercalates with double-stranded DNA: A gel-mobility-shift assay was employed to determine the intercalating properties of **2a** and **3d**.[17] This enables evaluation of the effect of ligand L in the $[Au_m(C^N^C)_mL]^{n+}$ class of compounds upon the DNA-binding affinities. A 100-base-pair DNA ladder treated with **2a**, **3d**, or ethidium bromide (EB, DNA intercalator) as well as a control were resolved by agarose-gel electrophoresis (Figure 9). Only samples that included EB or **2a** exhibited a tailing effect. This is due to the intercalation of these complexes with the DNA, which causes DNA elongation. The mobility of the bound DNA is lower than that of the free DNA. In contrast, **3d** did not cause this tailing effect, indicating that this compound does not bind to DNA by intercalation. By using viscosity analysis we confirmed that **2a** is a metallointercalator.[18] Addition of either EB or **2a** increased the viscosity of the DNA by increasing its hydrodynamic length, however, both Hoechst 33342 (a minor-groove binder) and **3d** failed

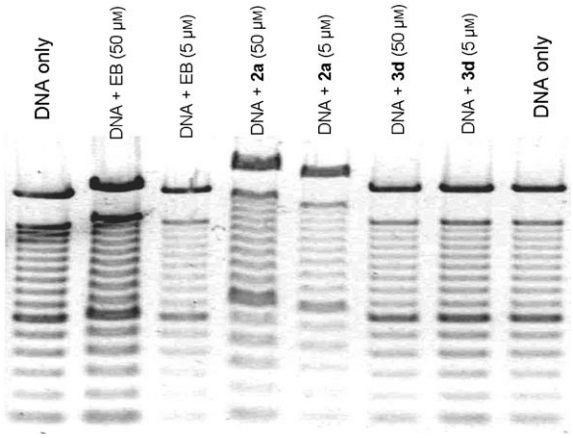

Figure 9. Gel electrophoresis of 100-bp DNA ladder on a 1.5% (w/v) agarose gel showing the mobility of DNA (50 μM bp^{-1}) in the absence or presence of ethidium bromide (EB), **2a**, or **3d**.

to lengthen the DNA and did not cause any changes in DNA viscosity (Figure S16).

Compound 2a is a potential telomerase inhibitor: Increased telomerase activity is observed in cancer cells, but not in normal cells, making telomerase an important target for chemotherapeutic intervention.[19] It has been reported that DNA intercalators enhance the assembly of G-quadruplexes. Consequently, we employed native polyacrylamide gel electrophoresis (PAGE) to examine the ability of **2a** to intercalate with DNA and induce the formation of intramolecular G-quadruplexes from oligonucleotide TR2 [5′-TACAGATAG(TTAGGG)$_2$TTA-3′]. As depicted in Figure 10, treatment of TR2 oligonucleotide with 6 μM **2a** resulted in dimeric (D) and tetrameric (T) G-quadruplex formations. As a comparison, 6 μM [Pt(terpy)Cl]Cl also induced formation of both G-quadruplex structures. This suggests that [Au(C^N^C)(1-methylimidazole)]$^+$ may be viewed as an analogue of [Pt(terpy)L]$^+$ from the perspective of DNA intercalation and potential telomerase inhibition.

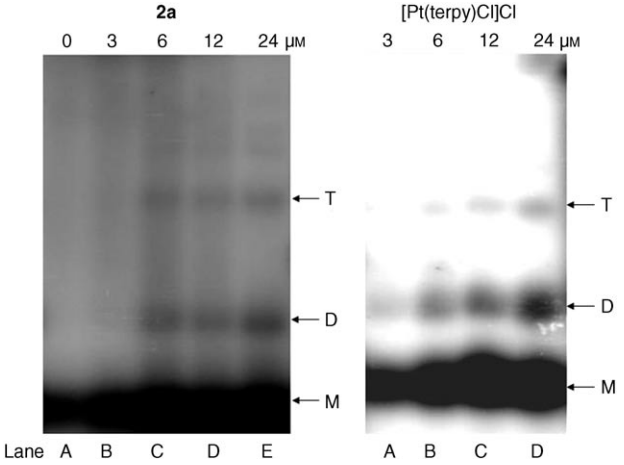

Figure 10. Compound **2a**- and [Pt(terpy)Cl]Cl-assisted assembly of G-quadruplexes from oligonucleotides resolved by native PAGE. **2a** and [Pt(terpy)Cl]Cl were incubated with oligonucleotide TR2 (8 μM) at 20°C in Tris buffer (10 mM, pH 8.0) containing EDTA (1 mM) and KCl (100 mM). Major bands are identified as monomer (M), dimer (D), and tetramer (T) compared with previous literature report.[25]

S-phase cell-cycle arrest: To determine whether cellular DNA is a major target of the gold(III) compounds, we studied the cell-cycle profiles of **2a**- or **3d**-treated cancer cells. Cell-cycle analysis was performed by using flow cytometry to assess the DNA content of cells stained with propidium iodide. This enables quantification of the total cellular populations in the different phases of the cell cycle (G0/G1, S, and G2/M). The flow-cytometric data for SUNE1 cells treated with cisplatin, **2a**, or **3c** is presented in Figure 11a. Treatment of cells with **2a** (12 μM, IC_{50} value) for 24 or 48 h enhanced cell-cycle arrest at the S phase (Figure 11c), the stage within which most DNA replication occurs.[20] As expected, the DNA-damaging agent cisplatin also significantly induced S-phase arrest, resulting in a concomitant decrease in the G1-phase population (Figure 11b). These results suggest that **2a** may induce apoptosis by inhibition of DNA replication. Conversely, treatment with **3d** did not significantly affect the cell cycle after 24- or 48-h incubation (Figure 11d). Apparently, different mechanisms are employed by compounds **2a** and **3d** to affect their cytotoxicities.

Conclusion

A series of stable cyclometalated gold(III) compounds [Au$_m$(C^N^C)$_m$L]$^{n+}$ (m=1–3; n=0–3; HC^N^CH=2,6-diphenylpyridine) was synthesized and found to exhibit potent cytotoxicity toward a panel of cancer cell lines, including a cisplatin-resistant variant. Modification of the auxiliary ligand (L) of this system significantly affects the biological activities, including the mechanism of cytotoxicity and DNA-binding affinity.

We demonstrated that this [Au$_m$(C^N^C)$_m$L]$^{n+}$ system can act as cytotoxic agents, metallointercalators, and potential telomerase inhibitors through ligation of nontoxic N-donor (**2**) ligands. Compounds **2a–c** exhibit general cytotoxic activities towards different types of cancer cells similar to those displayed by cisplatin and a number of previously reported gold(III) compounds. By using [Au(C^N^C)(1-methylimidazole)]$^+$ (**2a**) as a model compound, we showed that this class of compounds can induce apoptosis in cancer cells and binds strongly to DNA by intercalation. These compounds can also induce cell-cycle arrest in the S phase. Taken together, these results suggest that DNA binding may be a crucial event for the observed cytotoxicity of this class of molecules.

Ligation of the [Au(C^N^C)]$^+$ unit(s) to various kinds of phosphine ligands resulted in the formation of a series of mono- (**3a**), bi- (**3b-g**), and tri- (**3h**) nuclear gold(III) compounds. With higher solution stability than the metal-free phosphine ligands, these gold(III) compounds exhibit potent ligand-mediated cytotoxicity. Thus, the [Au(C^N^C)]$^+$ moiety can be regarded as a vehicle to carry highly cytotoxic phosphine ligands to cancer cells. Unlike the aforementioned [Au(C^N^C)]$^+$-mediated cytotoxic compound **2a**, [Au$_2$(C^N^C)$_2$(μ-dppp)]$^{2+}$ (**3d**) has neither significant DNA-binding activity nor the ability to induce cell-cycle arrest.

The structural similarities to the classical metallointercalator [Pt(terpy)Cl]$^+$, the enhanced stabilization of the electrophilic gold(III) ion by the dianionic C^N^C ligand, and the ease with which the [Au$_m$(C^N^C)$_m$L]$^{n+}$ system can be modified and even assembled into a polynuclear system (m=2 or 3) offers the possibility for a new class of stable gold(III) compounds with potentially medically important and tunable biological activities.

Experimental Section

Materials: All chemicals, unless otherwise noted, were purchased from Sigma–Aldrich. All solvents were purified according to conventional methods.

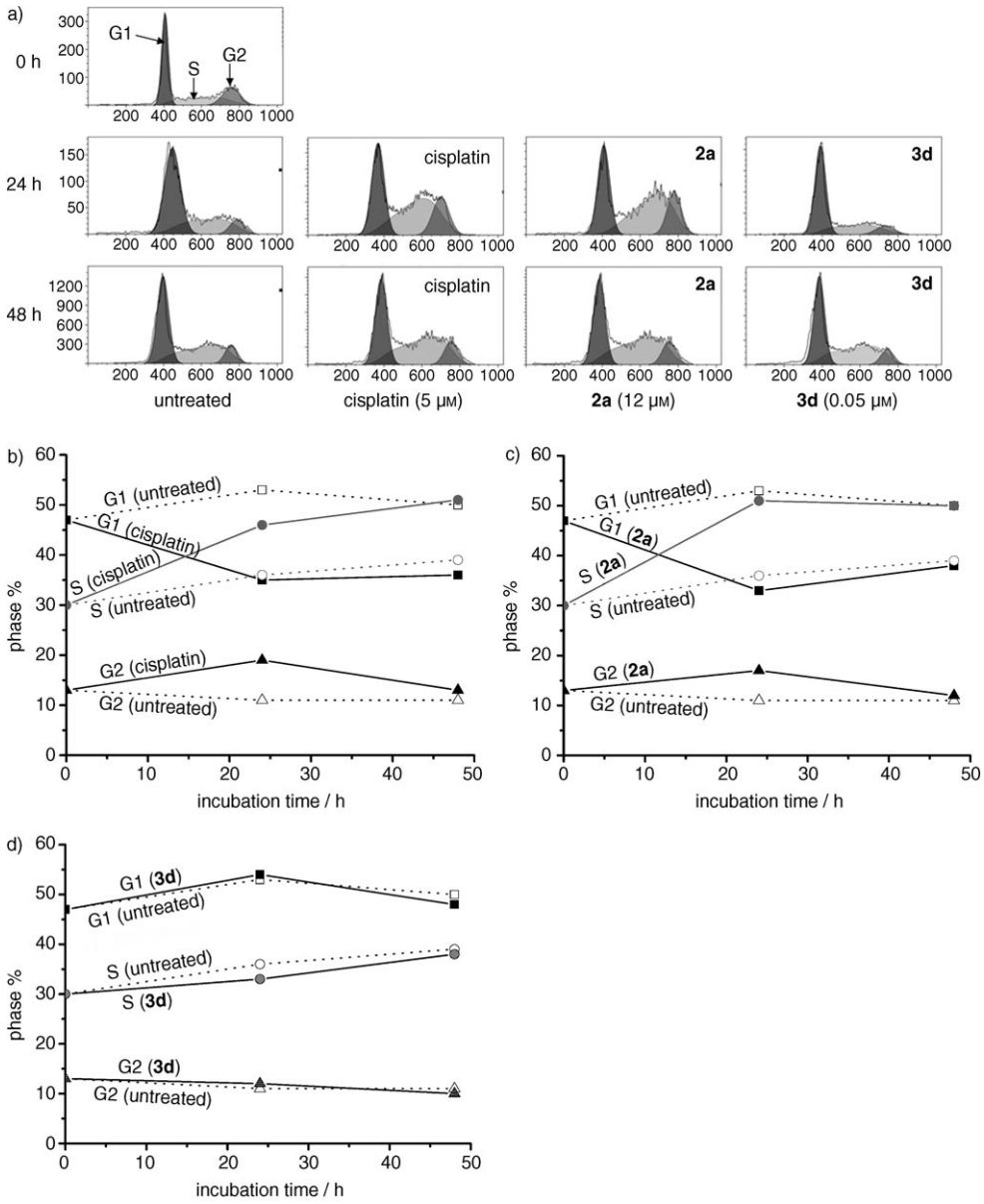

Figure 11. Induction of cell-cycle arrest in the SUNE1 cancer cells after treatment with gold(III) compounds. a) Untreated SUNE1 cells, and SUNE1 cells treated with cisplatin (5 μM), **2a** (12 μM), or **3d** (0.05 μM) were collected at different times of incubation (24 or 48 h) and subjected to flow-cytometry analysis. Graphical representation of the fluorescence-assisted cell-sorting (FACS) data, including the % of G1-phase cells (G1), S-phase cells (S), and G2-phase cells (G2) treated with cisplatin (b), **2a** (c), or **3d** (d).

Calf-thymus DNA (ctDNA) was purified by phenol/chloroform extraction. Polynucleotides, $[poly(dA–dT)]_2$ and $[poly(dG–dC)]_2$ were used as received. The 100-bp DNA ladder was obtained from Amersham Pharmacia Biotech. Cell Proliferation Kit I (MTT) and Annexin V–Fluos Staining Kit were purchased from Roche. Human cervical epithelioid carcinoma cells (HeLa) were obtained commercially from American Type Culture Collection (ATCC). Human nasopharyngeal carcinoma cells (SUNE1 and its cisplatin-resistant variant, CNE1) were derived from poorly differentiated NPC in Chinese patients,[21] and were generously provided by Prof. S. W. Tsao (Department of Anatomy, The University of Hong Kong, Hong Kong). Cell-culture flasks and 96-well microtitre plates were purchased from Nalge Nunc. Culture medium, other medium constituents, and phosphate-buffered saline (PBS) were from Gibco BRL.

Instrumentation: ^{1}H NMR spectra were recorded by using a DPX-300 or 400 Bruker FT-NMR spectrometer with chemical shift (in ppm) relative to tetramethylsilane. Mass spectra (FAB and EI) were recorded by using a Finnigan MAT95 mass spectrometer using 3-nitrobenzyl alcohol (NBA) as matrix. ESI mass spectra were recorded by using a Finnigan LCQ mass spectrometer. Gold analysis was undertaken by using an Agilent 7500 inductively coupled plasma mass spectrometer. All absorption spectra were recorded by using a Perkin–Elmer Lambda 900 UV/Vis spectrophotometer. Cyclic voltammetry was recorded by using a PAR Protentiostat/Galvanostat Model 273A. Elemental analyses were performed by the Institute of Chemistry at Chinese Academy of Sciences, Beijing. Viscosity experiments were performed by using a Cannon–Manning semimicro viscometer immersed in a thermostated water bath maintained at 27 °C. Flow-cytometric analysis was performed by using a Coulter EPICS flow cytometer (Coulter, Miami, FL) equipped with 480 long, 525 band, and 625 long-pass mirrors.

Syntheses

2,6-Dinaphthylpyridine:[7] Potassium *tert*-butoxide (4.0 g, 35.2 mmol) was added to a stirred solution of 2-acetonaphthaone (3 g, 17.6 mmol) in THF (20 mL) under a N_2 atmosphere. After stirring for 2 h, a solution of 3-(dimethylamino)-1-(2-naphthyl)-2-propen-1-one (4.0 g, 17.6 mmol) in THF (20 mL) was added dropwise. The reaction was stirred for 15 h. Ammonium acetate (13.6 g, 176 mmol) and acetic acid (20 mL) were added; the resulting mixture was refluxed for 2 h. After removal of solvent, water (30 mL) was added and the aqueous solution was extracted twice with CH_2Cl_2 (3×30 mL). The combined organic extracts were dried over magnesium sulfate and filtered through silica gel. The solvent was evaporated to give a pale-yellow solid (52%). ^{1}H NMR (300 MHz, $[D_6]$DMSO): δ = 8.65 (s, 2H), 8.37 (dd, J = 6.9, 1.8 Hz, 2H), 8.03–7.98 (m, 4H), 7.92–7.88 (m, 5H), 7.55–7.52 ppm (m, 4H); EIMS: m/z: 331 [M^+].

The syntheses and characterization of **1**, **2a**, and **3a–c** have been reported previously.[5b]

*[Au(C^N^C)Py]ClO$_4$ (**2b**-(ClO$_4$))*: The procedure was similar to that for **2a** except that pyridine was used. Yield: 76%. ^{1}H NMR (300 MHz, $[D_6]$DMSO): δ = 9.25 (d, J = 5.1 Hz, 2H), 8.48 (t, J = 7.8 Hz, 1H), 8.30 (t, J = 8.1 Hz, 1H), 8.10–8.05 (m, 4H), 7.98–7.96 (m, 2H), 7.39–7.32 (m, 4H), 6.73–6.71 ppm (m, 2H); UV/Vis (DMSO): λ_{max} (logε) = 265 (4.49), 283 (4.33, sh), 311 (4.18), 384 (3.73), 404 nm (3.71); FAB-MS: m/z: 505 [M^+]: elemental analysis calcd (%) for $C_{22}H_{16}N_2O_4ClAu$: C 43.69, H 2.67, N 4.63; found: C 43.53, H 2.57, N 4.77.

*[Au$_2$(C^N^C)$_2$(μ-Im)](ClO$_4$) (**2c**-(ClO$_4$))*: The procedure was similar to that for **2a** except that imidazole was used. Yield: 56%. ^{1}H NMR (400 MHz, [D$_6$]DMSO): δ = 8.64 (s, 1H), 8.27 (t, J = 8.0 Hz, 2H), 8.04 (d, J = 8.0 Hz, 4H), 7.96 (d, J = 6.6 Hz, 4H), 7.84 (s, 2H), 7.45–7.35 (m, 8H), 7.06 ppm (d, J = 7.1 Hz, 4H); UV/Vis (DMSO): λ_{max} (logε) = 263 (4.37), 281 (4.20, sh), 311 (4.04), 386 (3.62), 403 nm (3.59); FAB-MS: m/z: 919 [M^+]; elemental analysis calcd (%) for C$_{37}$H$_{25}$N$_4$O$_4$ClAu$_2$: C 43.61, H 2.47, N 5.50; found: C 43.31, H 2.46, N 5.47.

*[Au$_2$(C^N^C)$_2$(μ-dppp)](CF$_3$SO$_3$)$_2$ (**3d**-(CF$_3$SO$_3$)$_2$)*: The procedure was similar to that for **3b** except that 1,2-bis(diphenylphosphino)propane (dppp) was used. Yield: 59%. ^{1}H NMR (300 MHz, [D$_6$]DMSO): δ = 8.21 (t, J = 8.0 Hz, 2H), 7.94–7.88 (m, 12H), 7.61–7.46 (m, 16H), 6.91 (t, J = 7.3 Hz, 4H), 6.50 (t, J = 7.4 Hz, 4H), 6.10 (d, J = 7.5 Hz, 4H), 3.78 (s, 4H), 3.47 ppm (s, 2H); UV/Vis (DMSO): λ_{max} (logε) = 264 (4.68), 308 (4.23, sh), 389 (3.81), 403 nm (3.78); FAB-MS: m/z: 1414 [M^+]; elemental analysis calcd (%) for C$_{63}$H$_{48}$F$_6$N$_2$O$_6$P$_2$S$_2$Au$_2$: C 48.41, H 3.10, N 1.79; found: C 48.22, H 3.08, N 1.95.

*[Au$_2$(C^N^C)$_2$(μ-dppb)](CF$_3$SO$_3$)$_2$ (**3e**-(CF$_3$SO$_3$)$_2$)*: The procedure was similar to that for **3b** except that 1,2-bis(diphenylphosphino)butane (dppb) was used. Yield: 44%. ^{1}H NMR (400 MHz, [D$_6$]DMSO): δ = 8.22 (t, J = 8.0 Hz, 2H), 7.96–7.93 (m, 12H), 7.75 (d, J = 7.8 Hz, 4H), 7.56–7.46 (m, 12H), 7.07 (t, J = 7.4 Hz, 4H), 6.69 (t, J = 7.3 Hz, 4H), 6.21 ppm (d, J = 7.6 Hz, 4H); UV/Vis (DMSO): λ_{max} (logε) = 261 (4.73), 308 (4.21, sh), 387 (3.72), 402 nm (3.68); FAB-MS: m/z: 1428 [M^+]; elemental analysis calcd (%) for C$_{64}$H$_{50}$F$_6$N$_2$O$_6$P$_2$S$_2$Au$_2$: C 48.74, H 3.20, N 1.78; found: C 49.47, H 3.31, N 1.77.

*[Au$_2$(C^N^C)$_2$(μ-dpppe)](CF$_3$SO$_3$)$_2$ (**3f**-(CF$_3$SO$_3$)$_2$)*: The procedure was similar to that for **3b** except that 1,2-bis(diphenylphosphino)pentane (dpppe) was used. Yield: 47%. ^{1}H NMR (300 MHz, [D$_6$]DMSO): δ = 8.28 (t, J = 8.0 Hz, 2H), 8.05 (dd, J = 1.8, 6.1 Hz, 4H), 7.93–7.87 (m, 12H), 7.64–7.49 (m, 4H), 7.53–7.49 (m, 8H), 7.18 (t, J = 7.4 Hz, 4H), 6.83 (t, J = 7.8 Hz, 4H), 6.26 (d, J = 6.9 Hz, 4H), 2.06 (d, J = 3.9 Hz, 2H), 1.78 ppm (s, 8H); UV/Vis (DMSO): λ_{max} (logε) = 262 (4.78), 280 (4.52, sh), 308 (4.29, sh), 385 (3.83), 403 nm (3.80); FAB-MS: m/z: 1441 [M^+]; elemental analysis calcd (%) for C$_{65}$H$_{52}$F$_6$N$_2$O$_6$P$_2$S$_2$Au$_2$: C 49.07, H 3.29, N 1.76; found: C 48.94, H 3.32, N 1.78.

*[Au$_2$(C^N^C)$_2$(μ-dpph)](CF$_3$SO$_3$)$_2$ (**3g**-(CF$_3$SO$_3$)$_2$)*: The procedure was similar to that for **3b** except that 1,2-bis(diphenylphosphino)hexane (dpph) was used. Yield: 47%. ^{1}H NMR (300 MHz, [D$_6$]DMSO): δ = 8.28 (t, J = 8.0 Hz, 2H), 8.05 (dd, J = 1.9, 6.2 Hz, 4H), 7.99–7.91 (m, 12H), 7.64–7.48 (m, 12H), 7.20 (t, J = 7.4 Hz, 4H), 6.85 (t, J = 7.5 Hz, 4H), 6.28 ppm (d, J = 7.7 Hz, 4H); UV/Vis (DMSO): λ_{max} (logε) = 261 (4.86), 282 (4.54), 307 (4.32), 387 (3.85), 402 nm (3.82); FAB-MS: m/z: 1455 [M^+]; elemental analysis calcd (%) for C$_{66}$H$_{54}$F$_6$N$_2$O$_6$P$_2$S$_2$Au$_2$: C 49.39, H 3.39, N 1.75; found: C 50.26, H 3.54, N 1.82.

*[Au$_3$(C^N^C)$_3$(μ-dpep)](CF$_3$SO$_3$)$_3$ (**3h**-(CF$_3$SO$_3$)$_3$)*: The procedure was similar to that for **3b** except that bis(diphenylphosphinoethyl)phenylphosphine (dpep) was used. Yield: 46%. ^{1}H NMR (500 MHz, [D$_6$]DMSO): δ = 8.07–8.02 (m, 3H), 7.91 (dd, J = 7.3, 5.7 Hz, 2H), 7.65–7.32 (m, 35H), 7.03 (t, J = 7.6 Hz, 4H), 6.89 (t, J = 7.5 Hz, 2H), 6.57 (br, 2H), 6.51 (t, J = 7.5 Hz, 4H), 6.33 (s, 2H), 6.04 (d, J = 7.6 Hz, 4H), 3.82–3.74 (m, 2H), 3.71–3.61 (m, 2H), 3.46–3.36 (m, 2H), 3.29–3.19 ppm (m, 2H); UV/Vis (DMSO): λ_{max} (logε) = 266 (4.75), 308 (4.42, sh), 392 (3.92), 403 nm (3.91); FAB-MS: m/z: 2111 [M^+]; elemental analysis calcd (%) for C$_{88}$H$_{66}$F$_9$N$_3$O$_9$P$_3$S$_3$Au$_3$: C 46.76, H 2.94, N 1.86; found: C 46.44, H 3.00, N 1.80.

*[Au(Ph-C^N^C)]Cl (**4a**)*: The procedure was similar to that for **1** except that 2,4,6-triphenylpyridine was used. Yield: 48%. ^{1}H NMR (400 MHz, [D$_6$]DMSO): δ = 8.31 (s, 2H), 8.12 (m, 4H), 7.71 (d, J = 7.1 Hz, 2H), 7.63 (m, 3H), 7.44 (t, J = 7.2 Hz, 2H), 7.34 ppm (t, J = 7.2 Hz, 2H); UV/Vis (DMSO): λ_{max} (logε) = 263 (4.59), 291 (4.63), 392 (3.56), 412 nm (3.56); FAB-MS: m/z: 537.5 [M^+]; elemental analysis calcd (%) for C$_{24}$H$_{19}$NOAuCl: C 50.59, H 3.36, N 2.46; found: C 50.51, H 3.28, N 2.46.

*[Au(Ph-C^N^C)(meim-1)]ClO$_4$ (**4b**-(ClO$_4$))*: The procedure was similar to that for **4a** except that 1-methylimidazole was used. Yield: 82%. ^{1}H NMR (400 MHz, [D$_6$]DMSO): δ = 8.84 (s, 1H), 8.37 (s, 2H), 8.21–8.17 (m, 4H), 7.83 (s, 1H), 7.68–7.64 (m, 4H), 7.40–7.38 (m, 4H), 6.99 ppm (m, 2H); UV/Vis (DMSO): λ_{max} (logε) = 265 (4.52), 291 (4.59), 303 (4.57, sh), 394 (3.60), 412 nm (3.59); FAB-MS: m/z: 584 [M^+]; elemental analysis calcd (%) for C$_{27}$H$_{21}$N$_3$O$_4$ClAu: C 47.42, H 3.10, N 6.14; found: C 46.98, H 3.04, N 6.14.

*[Au(Np-C^N^C)]Cl (**5a**)*: A mixture of KAuCl$_4$ (1.4 g, 3.70 mmol) and [(Np-C^N^C)HgCl] (2.0 g, 3.53 mmol) in CH$_3$CN was refluxed for 24 h to afford a greenish-yellow precipitate. The solid was filtered and washed with water and Et$_2$O. The solid was redissolved in hot CHCl$_3$ and filtered through celite. A crystalline yellow solid **5a** was obtained by evaporation of CHCl$_3$. Yield: 65%. ^{1}H NMR (500 MHz, [D$_7$]DMF): δ = 7.53 (t, J = 8.0 Hz, 2H), 7.61 (t, J = 8.0 Hz, 2H), 7.97 (dd, J = 8.0, 8.0 Hz), 8.28 (s, 2H), 8.35 (d, J = 8.4 Hz, 2H), 8.41 (t, J = 8.4 Hz, 1H), 8.28 ppm (s, 2H); UV/Vis (DMSO): λ_{max} (logε) = 274 (4.34), 289 (4.13, sh), 382 (3.84), 391 nm (4.45); FAB-MS: m/z: 561 [M^+]; elemental analysis calcd (%) for C$_{25}$H$_{15}$NClAu: C 53.45, H 2.69, N 2.49; found: C 53.28, H 2.66, N 2.55.

*[Au(Np-C^N^C)(meim-1)](CF$_3$SO$_3$) (**5b**-(CF$_3$SO$_3$))*: 1-Methylimidazole (10 equiv) was added to a solution of (**5a**) in a CH$_3$CN/CH$_2$Cl$_2$ mixture (40 mL, 1:1) with stirring. A clear yellow solution was obtained and excess NaOTf (10 equiv) was added. The mixture was stirred at RT for 12 h, filtered, and concentrated by using a rotary evaporator. Addition of Et$_2$O gave the crude product as a bright yellow solid, which was washed with water and Et$_2$O, and crystallized by diffusion of Et$_2$O into the CH$_3$CN solution. Yield: 46%. ^{1}H NMR (300 MHz, [D$_6$]DMSO): δ = 8.96 (s, 1H), 8.64 (s, 2H), 8.42 (t, J = 7.3 Hz, 1H), 3.31 (d, J = 8.1 Hz, 2H), 7.94 (d, J = 7.7 Hz, 4H), 7.79 (d, J = 4.1 Hz, 2H), 7.55 (d, J = 8.5 Hz, 4H), 7.43 (s, 2H), 4.07 ppm (s, 3H); UV/Vis (DMSO): λ_{max} (logε) = 275 (4.56), 297 (4.33, sh), 381 (3.89), 399 nm (4.01); FAB-MS: m/z: 608 [M^+]; elemental analysis calcd (%) for C$_{30}$H$_{21}$F$_3$N$_3$O$_3$SAu: C 47.56, H 2.79, N 5.55; found: C 47.23, H 2.76, N 5.49.

*[Au(Np-C^N^C)(PPh$_3$)](CF$_3$SO$_3$) (**5c**-(CF$_3$SO$_3$))*: The procedure was similar to that for **5b** except that triphenylphosphine (PPh$_3$) was used. Yield: 78%. ^{1}H NMR (400 MHz, [D$_7$]DMF): δ = 6.65 (s, 2H), 7.04 (d, J = 8.0 Hz, 2H), 7.44 (t, J = 8.1 Hz, 2H), 7.51 (t, J = 8.1 Hz, 2H), 7.79 (td, J = 7.7, 3.0 Hz, 6H), 7.91 (t, J = 7.4 Hz, 3H), 7.94 (d, J = 8.0 Hz, 2H), 8.28 (dd, J = 7.7, 13.5 Hz, 6H), 8.53 (m, 3H), 8.77 ppm (s, 2H); ^{31}P NMR (162 MHz, CD$_3$CN): δ = 39.02 ppm; UV/Vis (DMSO): λ_{max} (logε) = 280 (4.84), 298 (4.71, sh), 401 nm (4.38); FAB-MS: m/z: 788 [M^+]; elemental analysis calcd (%) for C$_{44}$H$_{30}$F$_3$NO$_3$PSAu: C 56.36, H 3.22, N 1.49; found: C 56.21, H 3.26, N 1.50.

*[Au$_2$(Np-C^N^C)$_2$(μ-dppm)](CF$_3$SO$_3$)$_2$ (**5d**-(CF$_3$SO$_3$)$_2$)*: The procedure was similar to that for **5b** except that 1,2-bis(diphenylphosphino)methane (dppm) was used. Yield: 80%. ^{1}H NMR (400 MHz, CD$_3$CN): δ = 3.45 (t, J = 7.2, 7.2 Hz, 2H), 6.33 (d, J = 8.0 Hz, 4H), 6.61 (s, 4H), 7.12 (t, J = 8.0 Hz, 4H), 7.24 (t, J = 8.0 Hz, 4H), 7.34 (br, 12H), 7.38 (d, J = 8.0 Hz, 4H), 7.43 (d, J = 8.0 Hz, 4H), 7.58 (s, 4H), 7.80 (t, J = 8.0 Hz, 2H), 8.26 ppm (br, 8H); ^{31}P NMR (162 MHz, CD$_3$CN): δ = 23.89 ppm; UV/Vis (DMSO): λ_{max} (logε) = 258 (5.01), 276 (5.01), 396 nm (4.41); FAB-MS: m/z: 1437 [M^+]; elemental analysis calcd (%) for C$_{77}$H$_{52}$F$_6$N$_2$O$_6$P$_2$S$_2$Au$_2$: C 53.30, H 3.02, N 1.61; found: C 53.38, H 3.05, N 1.60.

*[Au$_2$(Np-C^N^C)$_2$(μ-dppe)](CF$_3$SO$_3$)$_2$ (**5e**-(CF$_3$SO$_3$)$_2$)*: The procedure was similar to that for **5b** except that 1,2-bis(diphenylphosphino)ethane (dppe) was used. Yield: 75%. ^{1}H NMR (400 MHz, CD$_3$CN): δ = 4.57 (s, 4H), 6.45 (d, J = 8.0 Hz, 4H), 6.49 (s, 4H), 7.20 (t, J = 7.9 Hz, 4H), 7.43–7.49 (m, 16H), 7.58 (t, J = 7.5 Hz, 4H), 7.69 (d, J = 8.1 Hz, 4H), 7.75 (s, 4H), 7.96 (t, J = 8.0 Hz, 2H), 8.07 ppm (dd, J = 13.3, 7.2 Hz, 8H); ^{31}P NMR (162 MHz, CD$_3$CN): δ = 34.97 ppm; UV/Vis (DMSO): λ_{max} (logε) = 261 (5.01), 277 (5.03), 403 nm (4.46); FAB-MS: m/z: 1600 [M^+ + OTf] (OTf = CF$_3$SO$_3$), 1451 [M^+]; elemental analysis calcd (%) for C$_{78}$H$_{54}$F$_6$N$_2$O$_6$P$_2$S$_2$Au$_2$: C 53.56, H 3.11, N 1.60; found: C 53.65, H 3.10, N 1.62.

*[Au$_3$(Np-C^N^C)$_3$(μ-dpep)](CF$_3$SO$_3$)$_3$ (**5f**-(CF$_3$SO$_3$)$_3$)*: The procedure was similar to that for **5b** except that 1,2-bis(diphenylphosphinoethyl)-phenylphosphine (dpep) was used. Yield: 78%. ^{31}P NMR (162 MHz, CD$_3$CN): δ = 33.22 (d, J = 50.2 Hz), 36.83 ppm (t, J = 50.3 Hz); UV/Vis (DMSO): λ_{max} (logε) = 259 (5.21), 277 (5.24), 406 nm (4.74); FAB-MS: m/z: 2412 [M^+ + 2OTf], 2263 [M^+ + OTf], 2113 [M^+]; elemental analysis calcd (%) for C$_{112}$H$_{78}$F$_9$N$_3$O$_9$P$_3$S$_3$Au$_3$: C 52.53, H 3.07, N 1.64; found: C 52.58, H 3.02, N 1.59.

X-ray crystal-structure determination: X-ray crystal structures of **1**, **2b**-(ClO_4), **2c**-(ClO_4)·C_3H_7NO, **3d**-$(CF_3SO_3)_2$·4CH_3CN, **3h**-$(CF_3SO_3)_3$·CH_3CN·H_2O, **4a**·CH_3OH, **5a**, **5c**-(CF_3SO_3)·$CHCl_3$, **5d**-$(CF_3SO_3)_2$·H_2O, **5e**-$(CF_3SO_3)_2$·2Et_2O, and **5f**-$(CF_3SO_3)_3$·6$CHCl_3$·H_2O are shown in Figures S1, S2, 1–3, S3–S7, and 4, respectively. Compound **1** was grown by slow evaporation of DMSO; **2c**-$(ClO_4)_2$ was grown by slow diffusion of Et_2O into DMF solution; **2b**-(ClO_4), **3d**-$(CF_3SO_3)_2$·4CH_3CN, and **3h**-$(CF_3SO_3)_3$·CH_3CN·H_2O were grown by slow diffusion of Et_2O into CH_3CN solution; **4a**·CH_3OH was grown by slow evaporation of DMSO and MeOH; **5a**, **5c**-(CF_3SO_3)·$CHCl_3$, **5d**-$(CF_3SO_3)_2$·H_2O, **5e**-$(CF_3SO_3)_2$·2Et_2O, and **5f**-$(CF_3SO_3)_3$·6$CHCl_3$·H_2O were grown by slow diffusion of Et_2O into $CHCl_3$ solution.

Diffraction experiments were performed by using a MAR diffractometer using graphite monochromatized $Mo_{K\alpha}$ radiation ($\lambda = 0.71073$ Å). The images were interpreted and intensities were integrated by using the program DENZO.[22] The structure was solved by direct methods employing the SHELXS-97 program on a PC. Au was located according to the direct methods.[23] The positions of the other non-hydrogen atoms were found after successful refinement by full-matrix least-squares using the program SHELXL-97 on a PC. For **1**, one crystallographic asymmetric unit consists of half of a formula unit. In the final stage of least-squares refinement, all non-hydrogen atoms were refined anisotropically. For **2b**-(ClO_4), one crystallographic asymmetric unit consists of one formula unit, including perchlorate anion. In the final stage of least-squares refinement, disordered oxygen atoms were refined isotropically, other non-hydrogen atoms anisotropically. For **2c**-(ClO_4), one crystallographic asymmetric unit consists of one formula unit, including one perchlorate anion and one DMF molecule. In the final stage of least-squares refinement, all non-hydrogen atoms were refined anisotropically. For **3d**-$(CF_3SO_3)_2$·4CH_3CN, one crystallographic asymmetric unit consists of one formula. Two $[CF_3SO_3]^-$ anions were located. Four CH_3CN solvent molecules were also located. For **3h**-$(CF_3SO_3)_3$·CH_3CN·H_2O, one crystallographic asymmetric unit consists of one formula unit. Two $[CF_3SO_3]^-$ anions were clearly located; the third anion was disordered into two sets of positions. Restraints were applied to the disordered anion, assuming similar S–C, S–O, C–F, O···O, F···F bond lengths or distances, respectively; and thermal parameters of C, O, and F were assumed to be the same. One CH_3CN and one water oxygen were also located. For **4a**·CH_3OH, one crystallographic asymmetric unit consists of one formula unit. C(1) to C(8) were disordered by rotation along the Au–Cl bond. For **5a**, naphthaline and pyridine were constrained to be normal with bond lengths of 1.39 Å. For **5c**-(CF_3SO_3)·$CHCl_3$, there was one formula unit in the asymmetric unit. One $[CF_3SO_3]^-$ anion was located. One $CHCl_3$ solvent molecule was also located, which was partially (14%) disordered in the mode of rotation by the sharing carbon atom. Restraints were applied to the disordered $CHCl_3$, assuming similar C–Cl, Cl···Cl bond lengths or distances, respectively. For **5d**-$(CF_3SO_3)_2$·H_2O, two $[CF_3SO_3]^-$ anions and one water oxygen were located. Restraints were applied to the second anion, assuming similar S–O, C–F, 1,3-F···F, 1,3-O···O bond lengths or distances, respectively. For **5e**-$(CF_3SO_3)_2$·2Et_2O, there were 1.5 formula units in the asymmetric unit. Three $[CF_3SO_3]^-$ anions were located. Three Et_2O were also located. Restraints were applied to the anions and ethers, assuming similar S–C, S–O, C–F, 1,3-O···O, 1,3-F···F bond lengths or distances, respectively; and for ether assuming similar O–C, C–C, 1,3-O···C bond lengths or distances, respectively. For **5f**-$(CF_3SO_3)_3$·6$CHCl_3$·H_2O, three $[CF_3SO_3]^-$ anions were located; meanwhile, six $CHCl_3$ solvent molecules were also located besides one water oxygen. Due to high thermal parameters, restraints were applied to the anions and solvent molecules, assuming similar S–O, C–F, S–C, 1,3-S···F, 1,3-C···O, C–Cl, 1,3-Cl···Cl bond lengths or distances, respectively.

CCDC 278604 (**1**), 296116 (**2b**-(ClO_4)), 296117 (**2c**-(ClO_4)·C_3H_7NO), 296118 (**3d**-$(CF_3SO_3)_2$·4CH_3CN), 296120 (**3h**-$(CF_3SO_3)_3$·CH_3CN·H_2O), 278603 (**4a**·CH_3OH), 278605 (**5a**), 296121 (**5c**-(CF_3SO_3)·$CHCl_3$), 296122 (**5d**-$(CF_3SO_3)_2$·H_2O), 296123 (**5e**-$(CF_3SO_3)_2$·2Et_2O), and 298876 (**5f**-$(CF_3SO_3)_3$·6$CHCl_3$·H_2O) contain the supplementary crystallographic data for this paper. These data can be obtained free of charge from The Cambridge Crystallographic Data Centre via www.ccdc.cam.ac.uk/data_request/cif.

Cyclic voltammetry: Cyclic voltammagrams were recorded at a scan rate of 100 $mV s^{-1}$ with tetrabutylammonium hexafluorophosphate (0.1 M) in DMF as supporting electrolyte at RT. The working electrode was a glassy carbon electrode (Atomergic Chemetal V25, geometric area of 0.35 cm^2) and the counterelectrode was platinum gauze. A nonaqueous $Ag/AgNO_3$ reference electrode (0.1 M in MeCN) was contained within a separate compartment that was connected by means of fine sintered-glass disks to the solution to be measured. The ferrocenium/ferrocene was used as internal standard.

Cell culture: The human cell lines SUNE1 and CNE1 were maintained in RPMI 1640 medium. HeLa and HepG2 cells were maintained in a minimum essential medium (MEM) with Earle's balanced salts. All the media were supplemented with L-glutamine (2 mM) and fetal bovine serum (10%). Penicillin (100 $U mL^{-1}$) and streptomycin (100 $\mu g mL^{-1}$) were added to all media. Cultures were incubated at 37 °C in a humidified atmosphere of 5% CO_2/95% air, and were subcultured trice weekly.

Cytotoxicity evaluation: Assays of cytotoxicity were conducted in 96-well, flat-bottomed microtitre plates. The supplemented culture medium (90 μL) with cells (1×10^5 cells per mL) was added to the wells. Gold compounds were dissolved in the culture medium with 1% DMSO to concentrations of 0.5–100 μM, and the solutions were subsequently added to a set of wells. Control wells contained supplemented media with 1% DMSO (100 μL). The microtitre plates were incubated at 37 °C in a humidified atmosphere of 5% CO_2/95% air for a further 3 d. All the assays were run in parallel with a negative control (i.e., vehicle control) and a positive control, in which cisplatin was used as a cytotoxic agent.

Assessment of cytotoxicity was carried out by using a modified method of the Mosmann-based 3-(4,5-dimethylthiazol-2-yl)-2,5-diphenyltetrazolium bromide (MTT) assay.[9] At the end of each incubation period, MTT solution (10 μL, Cell Proliferation Kit I, Roche) was added into each well and the cultures were incubated further for 4 h at 37 °C in a humidified atmosphere of 5% CO_2/95% air. A solubilizing solution (100 μL) was added into the wells to lyse the cells and to solubilize the formazan complex formed. The microtitre plates were maintained in a dark, humidified chamber overnight. The formation of formazan was measured by using a microtitre plate reader at 550 nm and the percentages of cell survival were determined. The cytotoxicity was evaluated based on the percentage cell survival in a dose-dependent manner relative to the negative control.

Measurement of drug uptake: Cellular-uptake experiments were conducted according to the literature method with some modifications.[24] SUNE1 cells (5×10^4 cells) were seeded in 60-mm tissue-culture dishes with culture medium (2 mL/well) and incubated at 37 °C in an atmosphere of 5% CO_2/95% air for 24 h. The culture medium was removed and replaced with medium containing gold compound at 50 μM. After exposure to the gold compound for 2 h, the medium was removed and the cell monolayer was washed four times with ice-cold PBS. Milli-Q water (500 μL) was added and the cell monolayer was scraped off the culture dish. Samples (300 μL) were digested in 70% HNO_3 (500 μL) at 70 °C for 2 h then diluted 1:100 in water for inductively coupled plasma mass spectrometry (ICP-MS) analysis.

Absorption titration: A solution of **2a** (or **3a** or **3d**, 25 μM) in TBS/DMSO (9:1) solution (3000 μL) was placed in a thermostatic cuvette within a UV/Vis spectrophotometer and the absorption spectrum was recorded. Aliquots of a millimolar stock solutions of ctDNA, [poly(dA–dT)]$_2$, or [poly(dG–dC)]$_2$ were added to the sample solutions and absorption spectra were recorded after equilibration for 10 min per aliquot until saturation point was reached. The binding constant was determined by applying the Scatchard equation: $[DNA]/\Delta\varepsilon_{ap} = [DNA]/\Delta\varepsilon + [1/(\Delta\varepsilon \times K_b)]$, in which $\Delta\varepsilon_{ap} = |\varepsilon_A - \varepsilon_B|$ where $\varepsilon_A = A_{obs}/[complex]$, and $\Delta\varepsilon = |\varepsilon_B - \varepsilon_F|$ where ε_B and ε_F correspond to the extinction coefficients of the DNA-bound and -unbound complex, respectively.

Gel-mobility-shift assay: A 100-bp PCR product (50 $\mu M bp^{-1}$) was mixed with ethidium bromide and the gold(III) compounds in a 1:1 ratio of DNA-base-pair to small molecules. The mixtures were analyzed by gel electrophoresis using a 1.5% (w/v) agarose gel and tris-acetate-EDTA (TAE) buffer. The gel was stained after electrophoresis by immersion in a bath of ethidium bromide.

Viscosity evaluation: The method used by Cohen and Eisenberg was employed in this study.[18] Viscosity experiments were performed by using a viscometer immersed in a thermostated water bath maintained at 27 °C. Titrations of **2a**, **3d**, ethidium bromide, or Hoechst 33342 were carried out by the addition of concentrated stock solutions (1 μL) to the DNA sample in BPE buffer (6 mM Na_2HPO_4, 2 mM NaH_2PO_4, and 1 mM Na_2EDTA, pH 7.0) in the viscometer. DNA concentrations of approximately 1 mM (in base pairs) were used.

G-quadruplex assay: ^{32}P-labeled TR2 oligonucleotide [5′-TACAGATAG-$(TTAGGG)_2$TTA-3′] at a concentration of 8 μM was annealed by heating it in 10 mM Tris/1 mM EDTA (TBE) buffer containing KCl (100 mM, pH 8.0) to 95 °C for 10 min, followed by cooling to RT. Stock solution (2 μL) of **2a** and [Pt(terpy)Cl]Cl was added. The reaction mixture was incubated at RT for 1 h and then loaded onto a native acrylamide (12 %) vertical gel (1:19 bisacrylamide) in TBE buffer supplemented with KCl (20 mM). The reaction was terminated by addition of gel-loading buffer (8 μL, 30 % glycerol, 0.1 % bromophenol blue, 0.1 % xylene cyanol), and the subsequent solution (10 μL) was analyzed by native PAGE (12 %, the gel was pre-run for 30 min). Electrophoresis was performed at 4 °C in TBE buffer (pH 8.3) containing KCl (20 mM) for 15 h. The gels were dried and visualized under UV illumination.

Flow cytometry: SUNE cells (40000 cells) were cultured in 60 mm tissue-culture dishes with culture medium (2 mL/dish). Compound **2a** (12 or 60 μM) or culture medium containing 1 % DMSO was added to the dishes after 24 h incubation in a humidified atmosphere of 5 % CO_2/95 % air. The dishes were then incubated further for 48 or 72 h. Annexin V–FITC/propidium iodide staining was performed by following the Annexin V–Fluos Staining Kit user's manual provided by Roche.

Acknowledgements

We acknowledge support from The University of Hong Kong (University Development Fund) and the Area of Excellence Scheme (AoE/P-10/01) administered by the University Grants Committee (HKSAR, China). We are thankful to Drs. S.-C. Yan and D.-L. Ma for technical assistance.

[1] a) C. X. Zhang, S. J. Lippard, *Curr. Opin. Chem. Biol.* **2003**, *7*, 481; b) C. F. Shaw, III, *Chem. Rev.* **1999**, *99*, 2589; c) Z. Guo, P. J. Sadler, *Angew. Chem.* **1999**, *111*, 1610; *Angew. Chem. Int. Ed.* **1999**, *38*, 1512.

[2] a) M. Coronnello, E. Mini, B. Caciagli, M. A. Cinellu, A. Bindoli, C. Gabbiani, L. Messori, *J. Med. Chem.* **2005**, *48*, 6761; b) L. Giovagnini, L. Ronconi, D. Aldinucci, D. Lorenzon, S. Sitran, D. Fregona, *J. Med. Chem.* **2005**, *48*, 1588; c) L. Ronconi, L. Giovagnini, C. Marzano, F. Bettio, R. Graziani, G. Pilloni, D. Fregona, *Inorg. Chem.* **2005**, *44*, 1867; d) T. Yang, C. Tu, J. Zhang, L. Lin, X. Zhang, Q. Liu, J. Ding, Q. Xu, Z. Guo, *Dalton Trans.* **2003**, 3419; e) G. Marcon, S. Carotti, M. Coronnello, L. Messori, E. Mini, P. Orioli, T. Mazzei, M. A. Cinellu, G. Minghetti, *J. Med. Chem.* **2002**, *45*, 1672; f) L. Messori, F. Abbate, G. Marcon, P. Orioli, M. Fontani, E. Mini, T. Mazzei, S. Carotti, T. O'Connell, P. Zanello, *J. Med. Chem.* **2000**, *43*, 3541; g) P. Calamai, A. Guerri, L. Messori, P. Orioli, G. P. Speroni, *Inorg. Chim. Acta* **1999**, *285*, 309; h) R. G. Buckley, A. M. Elsome, S. P. Fricker, G. R. Henderson, B. R. C. Theobald, R. V. Parish, B. P. Howe, L. R. Kelland, *J. Med. Chem.* **1996**, *39*, 5208; i) H.-Q. Liu, T.-C. Cheung, S.-M. Peng, C.-M. Che, *J. Chem. Soc. Chem. Commun.* **1995**, 1787.

[3] a) C. T. Lum, Z. F. Yang, H. Y. Li, R. W.-Y. Sun, S. T. Fan, R. T. P. Poon, M. C. M. Lin, C.-M. Che, H. F. Kung, *Int. J. Cancer* **2006**, *118*, 1527; b) Y. Wang, Q.-Y. He, C.-M. Che, J.-F. Chiu, *Proteomics* **2006**, *6*, 131; c) Y. Wang, Q.-Y. He, R. W.-Y. Sun, C.-M. Che, J.-F. Chiu, *Cancer Res.* **2005**, *65*, 11553; d) R. W.-Y. Sun, W.-Y. Yu, H. Sun, C.-M. Che, *ChemBioChem* **2004**, *5*, 1293; e) C.-M. Che, R. W.-Y. Sun, W.-Y. Yu, C.-B. Ko, N. Zhu, H. Sun, *Chem. Commun.* **2003**, 1718.

[4] L. S. Hollis, S. J. Lippard, *J. Am. Chem. Soc.* **1983**, *105*, 4293.

[5] a) V. W.-W. Yam, K. M.-C. Wong, L.-L. Hung, N. Zhu, *Angew. Chem.* **2005**, *117*, 3167; *Angew. Chem. Int. Ed.* **2005**, *44*, 3107; b) K.-H. Wong, K.-K. Cheung, M. C.-W. Chan, C.-M. Che, *Organometallics* **1998**, *17*, 3505.

[6] a) K. Becker, C. Herold-Mende, J. J. Park, G. Lowe, R. H. Schirmer, *J. Med. Chem.* **2001**, *44*, 2784; b) G. Lowe, A. S. Droz, T. Vilaivan, G. W. Weaver, J. J. Park, J. M. Pratt, L. Tweedale, L. R. Kelland, *J. Med. Chem.* **1999**, *42*, 3167; c) G. Arena, L. M. Scolaro, R. F. Pasternack, R. Romeo, *Inorg. Chem.* **1995**, *34*, 2994; d) J. C. Dewan, S. J. Lippard, W. R. Bauer, *J. Am. Chem. Soc.* **1980**, *102*, 858; e) K. W. Jennette, J. T. Gill, J. A. Sadownick, S. J. Lippard, *J. Am. Chem. Soc.* **1976**, *98*, 6159; f) K. W. Jennette, S. J. Lippard, G. A. Vassiliades, W. R. Bauer, *Proc. Natl. Acad. Sci. USA* **1974**, *71*, 3839.

[7] S. C.-F. Kui, Ph.D. Thesis, University of Hong Kong, **2005**.

[8] a) W. Lu, M. C. W. Chan, N. Zhu, C.-M. Che, C. Li, Z. Hui, *J. Am. Chem. Soc.* **2004**, *126*, 7639; b) A. J. Goshe, I. M. Steele, B. Bosnich, *J. Am. Chem. Soc.* **2003**, *125*, 444; c) V. W.-W. Yam, K. M.-C. Wong, N. Zhu, *J. Am. Chem. Soc.* **2002**, *124*, 6506.

[9] a) T. Mosmann, *J. Immunol. Methods* **1983**, *65*, 55; b) see, for example: S.-Y. Wong, R. W.-Y. Sun, N. P.-Y. Chung, C.-L. Lin, C.-M. Che, *Chem. Commun.* **2005**, 3544.

[10] K. H. Chi, W. K. Chan, D. L. Cooper, S. H. Yen, C. Z. Lin, K. Y. Chen, *Cancer* **1994**, *73*, 247.

[11] a) N. J. Sanghamitra, P. Phatak, S. Das, A. G. Samuelson, K. Somasundaram, *J. Med. Chem.* **2005**, *48*, 977; b) S. J. Berners-Price, P. J. Sadler, *Chem. Br.* **1987**, *23*, 541; c) S. J. Berners-Price, C. K. Mirabelli, R. K. Johnson, M. R. Mattern, F. L. McCabe, L. F. Faucette, C. M. Sung, S. M. Mong, P. J. Sadler, S. T. Crooke, *Cancer Res.* **1986**, *46*, 5486; d) R. M. Snyder, C. K. Mirabelli, R. K. Johnson, C. M. Sung, L. F. Faucette, F. L. McCabe, J. P. Zimmerman, M. Whitman, J. C. Hempel, S. T. Crooke, *Cancer Res.* **1986**, *46*, 5054.

[12] a) J. C. Reed, *Nat. Rev. Drug Discovery* **2002**, *1*, 111; b) D. W. Nicholson, *Nature* **2000**, *407*, 810.

[13] L. H. Hurley, *Nat. Rev. Cancer* **2002**, *2*, 188.

[14] D.-L. Ma, C.-M. Che, *Chem. Eur. J.* **2003**, *9*, 6133.

[15] C. V. Kumar, E. H. Asuncion, *J. Am. Chem. Soc.* **1993**, *115*, 8547.

[16] D.-L. Ma, T. Y.-T. Shum, F. Zhang, C.-M. Che, M. Yang, *Chem. Commun.* **2005**, 4675.

[17] E. C. Long, J. K. Barton, *Acc. Chem. Res.* **1990**, *23*, 271.

[18] B. Cohen, H. Eisenberg, *Biopolymers* **1969**, *8*, 45.

[19] J.-L. Mergny, J.-F. Riou, P. Mailliet, M.-P. Teulade-Fichou, E. Gilson, *Nucleic Acids Res.* **2002**, *30*, 839.

[20] a) E. L.-M. Wong, G.-S. Fang, C.-M. Che, N. Zhu, *Chem. Commun.* **2005**, 4578; b) E. A. Harrington, J. L. Bruce, E. Harlow, N. Dyson, *Proc. Natl. Acad. Sci. USA* **1998**, *95*, 11945.

[21] S. Y. Gu, W. P. Tang, Y. Zeng, E. W. Zhao, W. H. Deng, K. Li, *Chin. J. Cancer* **1983**, *2*, 270.

[22] DENZO: "*The HKL Manual—A description of programs DENZO, XDISPLAYF and SCALEPACK*", written by D. Gewirth, with the cooperation of the program authors Z. Otwinowski and W. Minor, **1995**, Yale University, New Haven (USA).

[23] G. M. Sheldrick, SHELX97, Programs for Crystal Structure Analysis (Release 97–2), University of Göttingen, Göttingen, Germany, **1997**.

[24] M. J. McKeage, S. J. Berners-Price, P. Galettis, R. J. Bowen, W. Brouwer, L. Ding, L. Zhuang, B. C. Baguley, *Cancer Chemother. Pharmacol.* **2000**, *46*, 343.

[25] H. Han, C. L. Cliff, L. H. Hurley, *Biochemistry* **1999**, *38*, 6981

Received: January 26, 2006
Published online: April 27, 2006

